Energy & Environmental Science

ROYAL SOCIETY OF CHEMISTRY

ANALYSIS

View Article Online
View Journal | View Issue

Cite this: *Energy Environ. Sci.*, 2022, **15**, 3583

Large-scale hydrogen production *via* water electrolysis: a techno-economic and environmental assessment†

Tom Terlouw, *[ab] Christian Bauer, *[a] Russell McKenna [cd] and Marco Mazzotti [b]

Low-carbon (green) hydrogen can be generated *via* water electrolysis using photovoltaic, wind, hydropower, or decarbonized grid electricity. This work quantifies current and future costs as well as environmental burdens of large-scale hydrogen production systems on geographical islands, which exhibit high renewable energy potentials and could act as hydrogen export hubs. Different hydrogen production configurations are examined, considering a daily hydrogen production rate of 10 tonnes, on hydrogen production costs, life cycle greenhouse gas emissions, material utilization, and land transformation. The results demonstrate that electrolytic hydrogen production costs of 3.7 Euro per kg H_2 are within reach today and that a reduction to 2 Euro per kg H_2 in year 2040 is likely, hence approaching cost parity with hydrogen from natural gas reforming even when applying "historical" natural gas prices. The recent surge of natural gas prices shows that cost parity between green and grey hydrogen can already be achieved today. Producing hydrogen *via* water electrolysis with low costs and low GHG emissions is only possible at very specific locations nowadays. Hybrid configurations using different electricity supply options demonstrate the best economic performance in combination with low environmental burdens. Autonomous hydrogen production systems are especially effective to produce low-carbon hydrogen, although the production of larger sized system components can exhibit significant environmental burdens and investments. Some materials (especially iridium) and the availability of land can be limiting factors when scaling up green hydrogen production with polymer electrolyte membrane (PEM) electrolyzers. This implies that decision-makers should consider aspects beyond costs and GHG emissions when designing large-scale hydrogen production systems to avoid risks coming along with the supply of, for example, scarce materials.

Received 29th March 2022,
Accepted 20th July 2022

DOI: 10.1039/d2ee01023b

rsc.li/ees

Broader context

Hydrogen is supposed to play an important role as low-carbon energy carrier and feedstock in decarbonized economies. Today, however, hydrogen production relies on fossil resources and generates substantial environmental burdens. Water electrolysis coupled with renewable energy sources (so-called "green hydrogen") represents an alternative, which causes low greenhouse gas (GHG) emissions. Geographical islands have a huge potential as hydrogen export hubs—due to the high capacity factors of wind and photovoltaic (PV) electricity generators in these areas, often low population densities, and thus low local demand. Large-scale hydrogen production represents an opportunity for their economic development. Comprehensive techno-economic and environmental life cycle assessments are required to evaluate potential hydrogen production clusters in such favorable locations. This paper explores this potential by determining overall costs and environmental burdens—such as the utilization of (potentially scarce) materials and land transformation—of optimized large-scale hydrogen production configurations *via* water electrolysis.

[a] *Technology Assessment Group, Laboratory for Energy Systems Analysis, Paul Scherrer Institute, 5232 Villigen PSI, Switzerland. E-mail: tom.terlouw@psi.ch, christian.bauer@psi.ch*
[b] *Institute of Energy and Process Engineering, ETH Zürich, Zürich 8092, Switzerland*
[c] *Chair of Energy Systems Analysis, Department of Mechanical and Process Engineering, ETH Zürich, Zürich 8092, Switzerland*
[d] *Laboratory for Energy Systems Analysis, 5232 Villigen PSI, Switzerland*

† Electronic supplementary information (ESI) available. See DOI: https://doi.org/10.1039/d2ee01023b

1 Introduction

Hydrogen is considered an important energy carrier for the deep decarbonization of the global energy system.[1–7] More specifically, hydrogen is expected to play a key role in the decarbonization of difficult to electrify sectors, such as the steel industry.[5,7] Hydrogen is mainly (98%) generated from

carbon-intensive energy sources nowadays, namely steam reforming of methane (76%) and coal gasification (22%), also known as gray and black hydrogen, respectively.[7] Importantly, hydrogen is only environmentally sustainable when using very low-carbon energy sources for its production *via* water electrolysis—*e.g.*, photovoltaic (PV), wind, or (very) low-carbon grid electricity—also referred to as green hydrogen.[8,9] Currently, only 2% of global hydrogen production originates from water electrolysis.[7]

Green hydrogen produced *via* water electrolysis has several advantages compared to alternative low-carbon hydrogen production pathways. It exhibits a very high purity with more than 99.9%,[10] thereby avoiding additional cleaning steps.[11–14] Further, electrolysis can provide grid balancing services converting "excess electricity" from wind and solar peaks to hydrogen when dynamic electrolysis operation is possible. Such production can therefore profit from low electricity prices potentially resulting in low hydrogen production costs.[11,12]

The costs of green hydrogen are, however, currently still high (up to 15 Euro per kg H_2[8,15,16]) compared to fossil fuel based hydrogen production pathways, mainly due to the high investment needed for the electrolyzer.[8,15,17,18] Further, there are large uncertainties regarding the future development and the associated learning curve of electrolyzers.[8,17] There is therefore a need for comprehensive cost assessments to determine current hydrogen production costs of green hydrogen, as well as to examine the point in time of reaching cost parity with gray hydrogen with "historical" costs around 1–2 Euro per kg H_2.[6,8,16,19,20] Further, environmental assessments are required to determine whether "green" hydrogen—produced exclusively by renewable electricity in autonomous system configurations—indeed exhibits low greenhouse gas (GHG) emissions, as well as to determine potential trade-offs coming along with the large-scale deployment of green hydrogen production systems.

There is a general agreement that energy systems and hydrogen production pathways should be assessed based on overall cost as well as environmental life cycle assessments (LCAs) methodologies, to identify economic and environmental trade-offs.[21,22] Methane reforming with carbon capture and storage (CCS)—*i.e.*, blue hydrogen—could be an important low-carbon hydrogen production pathway complementary to green hydrogen,[23] although recent LCAs show a very wide range of climate change impacts as a result of large variability regarding methane emissions from natural gas supply chains.[24–27] Green hydrogen most often exhibits lower climate change impacts compared to blue hydrogen, and is non-sensitive to fugitive methane emissions and associated uncertainties.[8,24,28–31] Green hydrogen therefore seems to be the best option when economically feasible. Several recent studies quantify hydrogen production costs and/or associated environmental burdens generated *via* water electrolysis.

For example, Christensen[15] quantified costs of hydrogen production considering different configurations using water electrolysis. Static electricity prices and capacity factors were applied to calculate hydrogen costs in Europe and the United States. Mallapragada *et al.*[32] quantified hydrogen costs for configurations coupled to PV and energy storage across the United States, and identified suitable locations to reach levelized costs lower than 2.5 $ per kg H_2. Palmer *et al.*[28] determined energy requirements and life cycle GHG emissions of large-scale hydrogen production *via* water electrolysis with solar PV as the main electricity source at a specific location. Nguyen *et al.*[11] provided a techno-economic analysis of grid-coupled hydrogen production configurations with decarbonised grid electricity supply, and therefore disregarded an environmental assessment.

This short overview demonstrates that previous works have several shortcomings in their economic and/or environmental analysis. First, they were limited to either hydrogen production costs, for example ref. 11, 15 and 32–35, or GHG emissions,[28] but none of them addressed the potentially conflicting goals of minimizing costs and life cycle GHG emissions of hydrogen production. In addition, future large-scale green hydrogen production could also approach environmental boundaries regarding material utilization[28,36,37] and land transformation. Second, hydrogen production costs and environmental burdens were usually quantified with static electricity prices and/or capacity factors, applied to wind and PV electricity generation. In reality, electricity prices and electricity generation from these renewables are highly location-specific, variable, and intermittent.[38,39] Third, previous work designed the hydrogen production configurations with static sizing methodologies, while the design of such hydrogen production systems could be optimized based on site-specific conditions to minimize hydrogen production costs and environmental burdens. And lastly, the assessment of large-scale hydrogen production hubs at favorable hydrogen production locations—such as geographical islands and coastal areas—is currently missing. We define favorable hydrogen production locations as geographical areas with a high capacity factor of renewable energy sources in combination with a substantial potential for their expansion as well as an easy accessible transportation network. In this way, hydrogen production on favorable locations might enable the decoupling from hydrogen demand. To the author's knowledge, no comprehensive work has examined these economic and environmental considerations of optimally designed large-scale hydrogen production systems on favorable hydrogen production locations so far, the contributions of this work can be summarized as follows:

- We provide an integrated techno-economic as well as environmental LCA of large-scale hydrogen production *via* water electrolysis considering different configurations: grid-connected, autonomous (*i.e.*, not connected to the electricity grid), hybrid as well as different sub-configurations.

- Current and future costs (year 2040) as well as environmental burdens of hydrogen production are quantified for favorable hydrogen production locations using a comprehensive sensitivity analysis. Five potentially favorable hydrogen production hubs are selected as case studies on European coastal areas/islands (Crete, Eigerøy, Tenerife, Western Isles, and Borkum).

- A mixed integer linear programming (MILP) optimization problem is developed to optimally design hydrogen production

systems for different hydrogen production configurations, considering a large set of (renewable) energy generators and technologies.

• An LCA is conducted on the hydrogen production configurations, to determine whether cost-optimal hydrogen production indeed exhibits low GHG emissions. Besides, life cycle impacts on land transformation and on a set of (potentially scarce) materials are quantified.

• A prospective economic as well environmental life cycle analysis is conducted applying a modification of the background LCA database using open-source Python package *premise*.[40]

• A potential upscaling of hydrogen production is examined, using a future renewable energy scenario, to determine whether such an upscaling leads to limitations regarding (scarce) materials, electricity consumption, and land transformation.

This work provides insights into cost-optimal configurations and operations, which should guide utilities and operators to install such systems. Further, this paper demonstrates trade-offs between low-cost and low-GHG emissions as well as potential barriers for upscaling hydrogen production *via* water electrolysis, which could be helpful for policy makers and system designers. The structure of this paper is as follows. Section 2 provides the methods. Next, Section 3 shows the results, and the discussion follows in Section 4. Finally, the conclusions are drawn in Section 5.

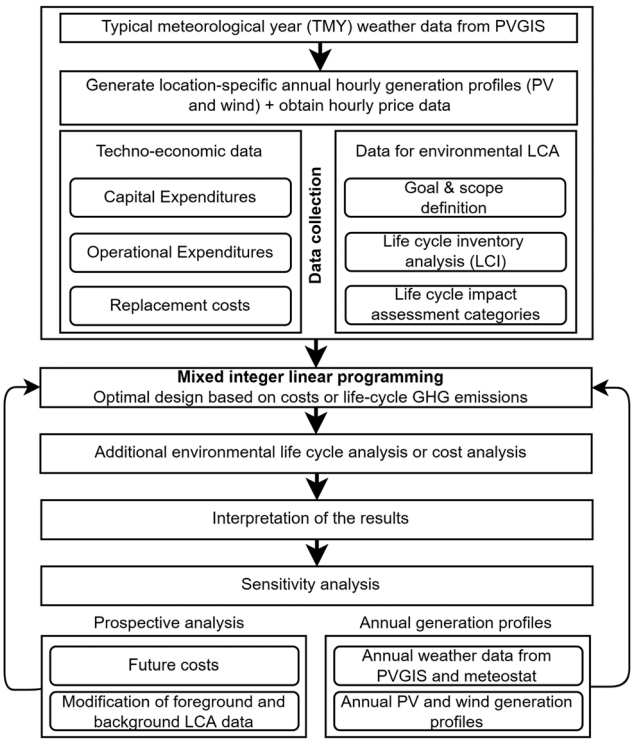

Fig. 1 Overview of methods used and their application.

2 Methods

Fig. 1 illustrates the methodology and procedure of this work. Hydrogen can be generated with different hydrogen production configurations using a wide set of (renewable) energy technologies in their system layout, see Section 2.1. We consider grid-connected configurations, hybrid, and autonomous configurations as well as two sub-configurations, which are described in Section 2.1.1–2.1.3. Data collection is performed to obtain weather, techno-economic, and environmental LCA data specifically for the considered case studies and system configurations. Next, a MILP problem is developed to optimally design hydrogen production systems with the use of annualized costs and/or life cycle GHG emissions; this is explained in Section 2.2 and in Section A of the ESI.† The outcome of the optimally sized system components and energy vectors are used to obtain environmental impacts other than impacts on climate change. Explanation of the main economic parameter is provided in Section 2.3. Additional assumptions regarding the environmental LCA data are presented in Section 2.4. The sensitivity analysis is discussed in Section D of the ESI,† using a prospective analysis as well as using the different annual generation profiles of renewable energy generators. And finally, the selected case studies are described in Section 2.5.

First, we assess individual large-scale hydrogen production configurations. Hydrogen production configurations of similar size (or most likely even larger) can be installed in the future and these could act as backbone of a future large-scale hydrogen economy. Second, the assessment of these large-scale hydrogen production configurations represents the indispensable basis for the system-analysis to determine barriers—regarding material utilization, land transformation, and electricity consumption—of this scale-up, which will be addressed in Section 3.2.3.

2.1 Hydrogen production: technologies and system configurations

Different configurations are considered to generate hydrogen. Literature focused on smaller hydrogen production systems so far, usually limited to a production rate of several hundreds kilograms up to several tonnes of hydrogen production per day. We, however, focus on cost-effective large-scale production for large-scale deployment, also to determine potential limitations such as material utilization and land transformation. The common feature of all these system configurations is to generate (on average) 10 tonnes of hydrogen per day. We believe that the upscaling of this technology requires a transition. We therefore chose to have a configuration that has a lower hydrogen production rate than traditional methods available, but higher than most techno-economic evaluations assumed so far.

The three considered hydrogen production configurations are explained in the following sections and are visualized in Fig. 2. A cradle-to-gate analysis is performed to supply hydrogen at the production gate. The system boundaries are chosen such that the production of all system components is included to produce and deliver hydrogen at 80 bar pressure.[28]

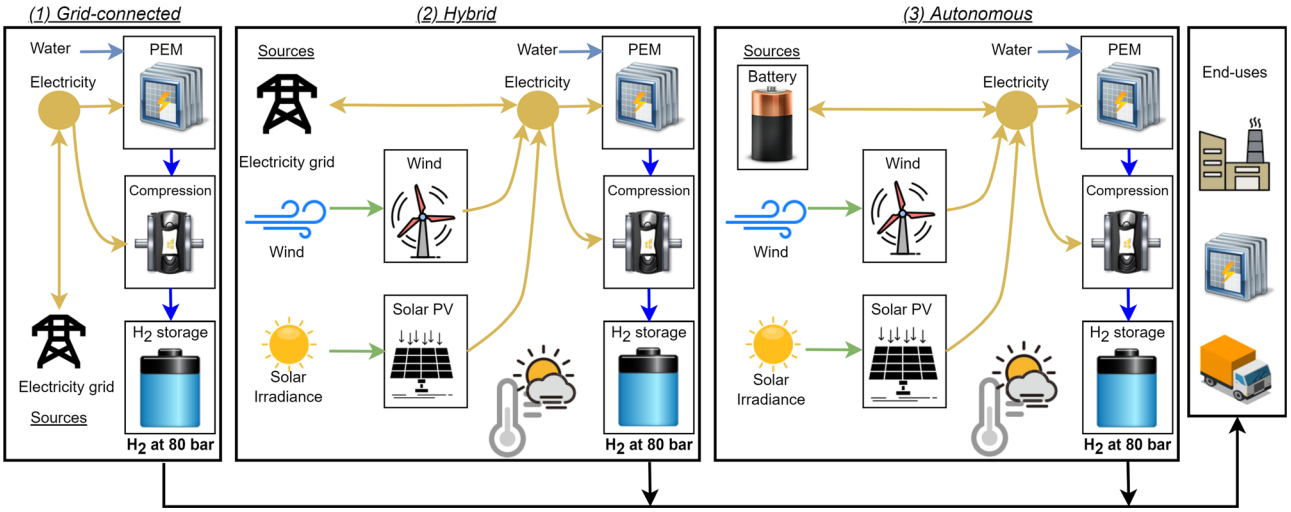

Fig. 2 Simplified illustration of the system boundaries of the three considered hydrogen production configurations: (1) grid-connected, (2) hybrid, and (3) autonomous, from left to right. Potential end uses are visualized, but are not considered in our system boundaries. For simplicity, desalination and deionisation of water are not visualized here, but are considered in our cost quantification and environmental LCA.

A polymer electrolyte membrane (PEM) electrolyzer is used to produce hydrogen and oxygen from water. PEM electrolyzers are well-known for their operational flexibility and fast response times as well as quick start-up times, and are therefore most appropriate to be considered in our configurations due to the possible integration of intermittent renewable electricity generators.[2,8,15] Water desalination is considered using reverse osmosis to treat seawater, to subsequently use the treated water in the PEM electrolyzer. Further, the electrolyzer consumes electricity to convert water to hydrogen and oxygen. The electricity for the entire hydrogen production system (water electrolysis, desalination plant, and subsequent hydrogen compression) can be delivered by different electricity sources: onshore wind, offshore wind, ground-mounted solar PV, the local electricity grid, and/or by discharging the battery. A compressor is installed to compress hydrogen from the output pressure of the electrolyzer (30 bar) to 80 bar. And lastly, hydrogen storage is considered to ensure a stable supply of hydrogen at the production gate.

2.1.1 Grid-connected. The grid-connected configuration consists of an electrolyzer connected to the national electricity grid. The main motivation for the selection of this system configuration is that selected (European) geographical locations are connected to their local or national electricity grid. The installed capacity of the electrolyzer will be determined by the targeted hydrogen production and our optimization problem, see Section A.1 of the ESI.† An energy management system determines the amount of electricity purchased to be used in the electrolyzer to produce hydrogen. The hydrogen production must equal 10 tonnes H_2 per day. Next, hydrogen is delivered to a hydrogen pressure tank considering one day hydrogen storage capacity (*i.e.*, 10 tonnes of hydrogen at 80 bar pressure). The optimization problem and associated constraints for this configuration are discussed in Section A and Section A.1 of the ESI,† respectively.

2.1.2 Hybrid. The hybrid configuration consists of a grid connection as well as a (possible) direct connection to renewable electricity sources, namely PV, onshore, and offshore wind electricity. The main motivation of this configuration is that hybrid systems can integrate (low-cost) renewable energy sources and can use the electricity grid as a (cheap) backup supply and storage buffer which might lead to lower costs and environmental burdens when coupled to a low GHG intensive electricity grid. Further, grid electricity can be used during time periods with low or even negative grid electricity prices and to allow for continuous electrolyzer operation reducing the required capacity. The system optimization finds the optimal solution (*i.e.*, hydrogen produced at lowest annualized costs or life cycle GHG emissions), and therefore determines the optimal electrolyzer capacity as well as PV and wind generation capacities. It is worth noting that PV solar and/or wind electricity generators are not required to be installed; this depends on the site-specific situation.

Multi-Si PV modules are selected, representing PV technology most often installed today.[41] The same hydrogen storage capacity is installed as for the grid-connected configuration. In this specific case, the grid can be used as a backup supply for times without wind or PV generation and as buffer—*i.e.*, a potential storage medium—when excess electricity is generated. An additional storage medium—*e.g.*, a battery—is therefore not considered in this configuration. The constraints for this configuration are provided in Section A.2 of the ESI.†

Hybrid-Green. Hybrid-Green is identical to the configuration as explained in Section 2.1.2. However, this sub-configuration, see Section A.2 of the ESI,† is constrained to a maximum amount of annual GHG emissions corresponding to the level of green hydrogen according to CertifHy with a specific carbon intensity of hydrogen equal to or lower than 4.4 kg CO_2-eq. per kg H_2.[42] For some configurations, such low carbon

intensity level cannot be reached and the configuration will be minimized on annual life cycle GHG emissions in this situation.

2.1.3 Autonomous. The autonomous configuration is a system layout, in which the electrolyzer is fully operated by locally available electricity from PV panels, onshore, and/or offshore wind turbines entirely disconnected from the electricity grid. The motivation for this configuration is that geographical islands or other remote locations could lack access to the national electricity grid; autonomous configurations are the only feasible solution in this situation. It is worth mentioning that curtailment of renewable electricity might be applied to balance power supply and demand.[43] This could, however, lead to non-used renewable electricity generation and to oversized energy technologies.

Again, our optimization problem decides whether to install PV modules and wind turbines, as well as installed capacity, to provide sufficient electricity to the electrolyzer. Compared to the other two configurations, we allow for additional flexibility in terms of hydrogen production: instead of a daily production rate of 10 tonnes H_2, this configuration exhibits a production of 50 tonnes H_2 within five days. It is worth mentioning that a less stringent constraint on the periodical hydrogen production quota most likely will result in less curtailment and oversized technologies. Logically, a larger storage medium is required for autonomous configurations and we therefore assume five days hydrogen storage capacity (50 tonnes H_2). Additionally, a battery can be installed to further increase flexibility, especially useful to shave PV and/or wind generation peaks and to reduce the installed capacity of the electrolyzer as such. A lithium nickel manganese cobalt oxide (NMC) battery is chosen as battery technology, since this represents mainstream battery technology nowadays and performs well on both costs and GHG emissions.[8,44,45] The optimization problem and associated constraints for this configuration are presented in Section A.3 of the ESI.†

Autonomous-grid injection. The autonomous-grid injection is the same configuration as explained in Section 2.1.3. However, it offers the possibility to inject excess electricity (produced by renewables) into the local grid electricity network to generate revenue, see Section A.3 of the ESI.† It is worth noting that grid demand charges and grid extension fees apply in this situation. Grid electricity absorption is not considered to avoid (possible) absorption of GHG intensive grid electricity. Indeed, this sub-configuration is not entirely autonomous, although it seems reasonable that excess renewable electricity generation can be sold at each timeslot to generate revenue to (for example) grid electricity operators or to the local industry.

2.2 Energy system optimization

Energy system optimization is used to optimally design and operate hydrogen production systems. To achieve this, we use MILP,[59] which is a well-known technique to optimally schedule and design energy systems.[45,60–63] The optimization problems are used to design the energy systems based on one year of system operation using an hourly resolution. The three energy system configurations are initially optimized on annualized costs, considering capital expenditures (CAPEX), operation costs, fixed operation & maintenance costs (O&M), and replacement costs. More explanation regarding the optimization problem as well as the constraints for each configuration are provided in Section A of the ESI.†

Besides being optimized regarding annualized costs, the system is also evaluated regarding life cycle GHG emissions—considering GHG emissions from the production of system components and system operation—and therefore a second objective has been defined, thus resulting in a multi-objective optimization problem. Pareto fronts are a well-known technique to illustrate trade-offs between annualized costs and GHG emissions of energy systems using multi-objective optimization.[45,62] More explanation regarding the procedure of the generation of the Pareto fronts is provided in Section A of the ESI.†

It is worth noting that the Pareto fronts are only generated for the hybrid hydrogen production system, since this configuration is both connected to the electricity grid (which can have a high GHG impact) and to renewable energy generators (with a low GHG impact), and it is therefore most sensitive regarding GHG emissions during energy system operation. Indeed, GHG emissions below these of the cost-optimal solution are also possible for the autonomous and the grid-connected configurations, but only to a comparatively minor extent.

2.3 Economic assessment

We include all costs during the lifetime of the different system configurations. To achieve this, investments, operation costs, fixed operation & maintenance as well as replacement costs are considered in our cost assessment. Table 1 provides an overview of the assumptions used in the techno-economic assessment for both the current situation and one (possible) mid-term future situation representative for year 2040. For the desalination plant, the costs are small and therefore the water costs are presented per kg H_2 considering the desalination plant in ref. 57. A project, or system, lifetime of 20 years has been assumed. Discount rates of hydrogen production systems usually vary between 5 and 8%,[5,15,55,56] and we therefore set the (real) discount rate to a conservative value of 7% in the main analysis. We, however, perform a sensitivity analysis regarding costs of technologies, lifetime as well as discount rates, since they are highly uncertain and depend on many factors.[53,64] The three costs scenarios—pessimistic, average, and optimistic—are provided in Table 1, where the lowest and highest technology and grid costs are represented in the optimistic and pessimistic scenario, respectively. Average grid electricity prices are case-specific and are provided in Table 2, and the electricity price profiles can be found in Section C of the ESI.†

The main economic indicator is the net costs per kilogram hydrogen produced (C_{H_2}), considering annualized investments ($C_{inv,an}$), operation costs (C_{op}) including revenues from grid electricity injection, fixed operation & maintenance costs (C_{om}) and annualized replacement costs ($C_{rep,an}$); they are divided by

Table 1 Techno-economic parameters used in our analysis. Using 1 $ = 0.9 Euro, 1 $ = 1 CHF, 1 GBP = 1.15 Euro. Average grid electricity prices are provided in Table 2. The CAPEX and efficiency of the electrolyzer are selected based on a wide set of literature sources presented by PIK.[46] Onshore and offshore wind costs are selected on an expert elicitation presented in ref. 47. In addition, solar PV and battery techno-economic parameters are selected based on reviews presented in ref. 8, 48 and 49. The cost figures refer to year 2020

Parameter	2020	2040 (pess.)	2040 (av.)	2040 (opt.)	Unit	Sources
Electrolyzer						
Efficiency	0.61	0.70	0.70	0.70	[-]	8, 46
Stack Lifetime	7	9	10	11	[Years]	8, 15, 50
CAPEX	1060	550	470	400	[Euro per kW]	8, 15, 46
O&M	2	2	2	2	[%]	15, 51
Balance of system	45	45	45	45	[Euro per kW]	8, 15
H_2 storage						
Lifetime	20	25	25	25	[Years]	8
CAPEX	460.0	280.0	240.0	200.0	[Euro per kg H_2]	8, 32
O&M	1	1	1	1	[%]	32
Compressor						
Lifetime	10	10	10	10	[Years]	52
CAPEX	2440	2440	2440	2440	[Euro per kW]	15
O&M	4	4	4	4	[%]	32
Wind offshore						
Lifetime	27	28	30	32	[Years]	8, 47
CAPEX	2700	2500	2000	1500	[Euro per kW_p]	8, 47
O&M	2.4	2.4	2.4	2.4	[%]	51
Wind onshore						
Lifetime	27	28	30	31	[Years]	8, 47
CAPEX	1400	1130	1000	860	[Euro per kW_p]	8, 47
O&M	2.4	2.4	2.4	2.4	[%]	51
Solar PV						
Lifetime	30	35	35	35	[Years]	8, 48
CAPEX	950	650	540	450	[Euro per kW_p]	8, 48
O&M	2	2	2	2	[%]	51
Battery						
Depth of discharge	0.93	0.93	0.93	0.93	[-]	8, 53
Roundtrip efficiency	0.91	0.91	0.91	0.91	[-]	8, 53
CAPEX (battery pack)	180	100	80	60	[Euro per kWh]	8, 49, 53
Lifetime (battery pack)	13	13	13	13	[Years]	8, 53
CAPEX (power unit)	140	60	60	60	[Euro per kW]	8, 53
Lifetime (power unit)	20	20	20	20	[Years]	44
O&M	10	10	10	10	[Euro per kW per a]	8, 53
Self disch. Rate	0.00054	0.00054	0.00054	0.00054	[per h]	54
General						
System lifetime	20	20	20	20	[Years]	8
Discount rate	0.07	0.08	0.07	0.05	[-]	5, 15, 52, 55, 56
Water desalination cost	0.018	0.018	0.018	0.018	[Euro per kg H_2]	57
Increase cost grid	n.a.	1.02	1.013	1.005	[per a]	58

the annual hydrogen production rate ($H_{2,total}$).

$$C_{H_2} = \frac{C_{op} + C_{inv,an} + C_{rep,an} + C_{om}}{H_{2,total}}. \quad (1)$$

2.4 Environmental assessment: life cycle assessment (LCA)

An LCA approach is applied to determine GHG emissions and potential environmental trade-offs associated to the implementation of large-scale hydrogen production configurations.[21] LCA is standardized by ISO 14040[72] and ISO 14044.[73] LCA has been commonly used in scientific literature to assess products or services over their entire life cycle to determine overall environmental impacts, preferably considering a wide set of environmental impact categories.[22] An attributional LCA approach has been applied and the LCA results are calculated with Brightway2.[74] We attribute all environmental impacts to hydrogen, since the economic value of oxygen from hydrogen production output is currently uncertain, but generally and

Table 2 Characteristics and generalization of selected case studies on the wind and PV solar availability,[65–69] grid electricity price,[70] and GHG intensity of the electricity grid.[71] CF = capacity factor, Av. = average., E. = electricity

	CF offshore wind (-)	CF onshore wind (-)	CF solar PV (-)	Av. grid E. price (Euro per kWh)	GHG intensity E. grid (kg CO_2-eq. per kWh)
Crete	0.39	0.33	0.20	0.064	0.747
Eigerøy	0.56	0.47	0.11	0.039	0.023
Borkum	0.59	0.52	0.13	0.038	0.542
Tenerife	0.49	0.43	0.20	0.048	0.387
Western Isles	0.56	0.47	0.10	0.049	0.342

comparatively small. The functional unit is defined as: "One kilogram hydrogen at 80 bar pressure with a purity of more than 99.9%, considering an (average) reference flow of 10 tonnes hydrogen production and storage per day". It is worth noting that the outputs of the cost optimization problems are used as input for the environmental LCA. In this way, the cost-optimal sizes of system components and system operation are considered in the LCA.

2.4.1 Life cycle inventory. Ecoinvent v3.7.1, system model "*Allocation, cut-off by classification*" is chosen as source of background LCA database.[71,75] Key components of the hydrogen production system are modeled as follows. Desalination of water is considered. Seawater is assumed to be treated with reverse osmosis, and afterwards deionised—considering the infrastructure and chemicals required (such as the resin)—to be used in the PEM electrolyzer. The electricity requirement for reverse osmosis amounts to 3.72 kWh m^{-3} water,[71] and it therefore has a minor contribution to the overall energy requirement of water electrolysis, around 0.1%.[57,76] Next, PEM electrolyzers generate hydrogen at around 30 bar pressure with an efficiency of 61% (lower heating value).[8,15,46] LCI of a PEM electrolyzer has been generated based on the work of Bareiß *et al.*[50] and is provided in Section B of the ESI.† A compressor is used to compress hydrogen from 30 bar to 80 bar to be stored in storage vessels. We find an electricity requirement for the compressor of 0.51 kWh per kg H_2.[15] Cylindrical vessels are considered with storage capacities of 10 tonnes H_2 and 50 tonnes H_2, respectively, corresponding to one day and five days H_2 of hydrogen production. We adopt the LCI of Palmer *et al.* regarding the storage vessels, where each vessel is able to store 527 kg H_2.[28] This leads to a total of 19 vessels made of stainless steel for 10 tonnes H_2 storage capacity. LCI of ground-mounted PV systems from the ecoinvent database has been updated based on Frischknecht *et al.*[77] LCI for the battery system is adopted from Schmidt *et al.*,[44] considering a recent update regarding energy consumption for battery production.[8] Other foreground LCI datasets are provided in Section B of the ESI.†

The IPCC 2013 GWP100a life cycle impact assessment method has been selected regarding climate change impacts. Further, we aggregate all "Transformation, from…" biosphere flows to obtain the square meters of land transformation for each system configuration, to determine the total amount of land transformation. Similarly, we aggregate biosphere flows for the following set of potentially scarce materials (selection based on Palmer *et al.*[28] and Terlouw *et al.*[36]) to determine their utilization (kilograms, in ground) in our system configurations: cobalt, iridium, platinum, titanium, lithium, tin, and silver.

2.4.2 Environmental performance. The selected environmental indicators correspond to the functional unit in terms of the amounts of environmental burdens generated per kilogram hydrogen production. For hybrid configurations, we do not take into account credits for avoided environmental burdens due to electricity injection into the grid for the following reasons. First, location specific electricity grid models would be required for determining the marginal suppliers to be substituted: such an analysis is beyond the scope of this study. Second, the goal of a hydrogen producer is to reduce GHG emissions generated at the hydrogen production site, and most likely not from the avoidance of indirect emissions generated in the electricity grid, since there are currently no specific regulations in place for such avoided GHG emissions. And lastly, additional grid electricity injection could lead to imbalances as well as additional pressure on the electricity grid. This could require capacity extensions of the grid, which inevitably leads to additional costs and environmental burdens; their quantification would also require a system perspective employing a power grid model.[78] We, however, provide an additional analysis to show the consequences of considering a credit for GHG emissions when excess electricity is injected into the electricity grid, see Section G.2 of the ESI.†

Further, the explanation of the sensitivity analyses regarding future hydrogen production costs, environmental impacts, and the optimal design on weather data is provided in Section D of the ESI.†

2.5 Selection of case studies

As discussed in the introduction, geographical islands as well as coastal areas often have the potential of electricity generation at low-costs, due to a high availability of wind and/or solar energy compared to the mainland. Further, geographical islands usually have comparably high availability of land and sea area to generate renewable electricity. Further, smaller islands often rather have low energy demand due to low population densities and lack of industrial activities. Besides, infrastructure for long-distance hydrogen transportation, *e.g.*, by ships, is potentially easier to deploy on geographical islands. And finally, large-scale hydrogen production offers the opportunity to establish new industries on islands, fostering the local community and its economic development. Geographical islands are typically dependent on fossil fuels imported from the mainland nowadays. Some European islands, for example Crete, Eigerøy and Western Isles, aim to maximize the self-sufficiency and establish distributed energy systems, while minimizing their reliance on non-renewable energy sources in order to reduce their overall environmental footprint and costs.[79] These initiatives usually integrate hydrogen as one of the main (future) energy carriers.

This paper therefore considers large-scale hydrogen production on five geographical islands in Europe, although is not limited to these islands. Europe has been chosen, since it is likely that the roll-out of large-scale hydrogen production will take place in Europe due to recently announced ambitious European climate policy.[80–82] Five geographical islands are selected in this study with different characteristics; Crete (Greece), Eigerøy (Norway), Tenerife (Spain), Western Isles (Scotland, UK), and Borkum (Germany). Crete and Tenerife are islands with a large availability of solar irradiation during the entire year, while Eigerøy, Borkum, and Western Isles are situated to the north of Europe and have a comparably high availability of wind energy sources during the entire year. Further, all countries have different characteristics regarding the GHG intensity of the electricity grid and the variability of grid electricity prices.

Fig. 3 Selected European geographical islands on a map.

An overview is provided in Section C of the ESI.† The selected case studies are drawn on a map in Fig. 3.

It is worth noting that onshore wind is a (very) constrained energy source and is already exploited on many geographical islands and coastal areas. We therefore add a constraint regarding the maximum installed capacity of onshore wind for hybrid and autonomous configurations. We consider a small potential (max. 10 MW) and larger onshore wind potential (max. 100 MW). Eigerøy (Norway) and Borkum (Germany) are assumed to have a low onshore wind potential due to the low availability of land area and earlier difficulties to implement wind power. Tenerife (Spain), Crete (Greece), and Western Isles (Scotland, UK) are assigned with a larger onshore potential due to the larger land availability on these geographical islands and coastal areas. The amount of land available for solar PV is also constrained, the procedure to account for that is provided in Section A of the ESI.†

Data collection and assumptions for future scenarios are presented in Table 1. Three cost scenarios are considered: pessimistic, average, and optimistic. The information and explanation of data sources and scenarios used is provided in Section E of the ESI.†

3 Results

All results are presented in the following sub-sections and are illustrated in Fig. 4–11. Table 3 shows the optimization outcome regarding the installed capacity of system components, renewable electricity curtailment, and the capacity factor of the electrolyzer. Weekly summer and winter operations of the hydrogen production system for the autonomous as well as the autonomous-grid injection configurations are provided in Section G.5 of the ESI.† Additional figures can be found in Section G of the ESI.†

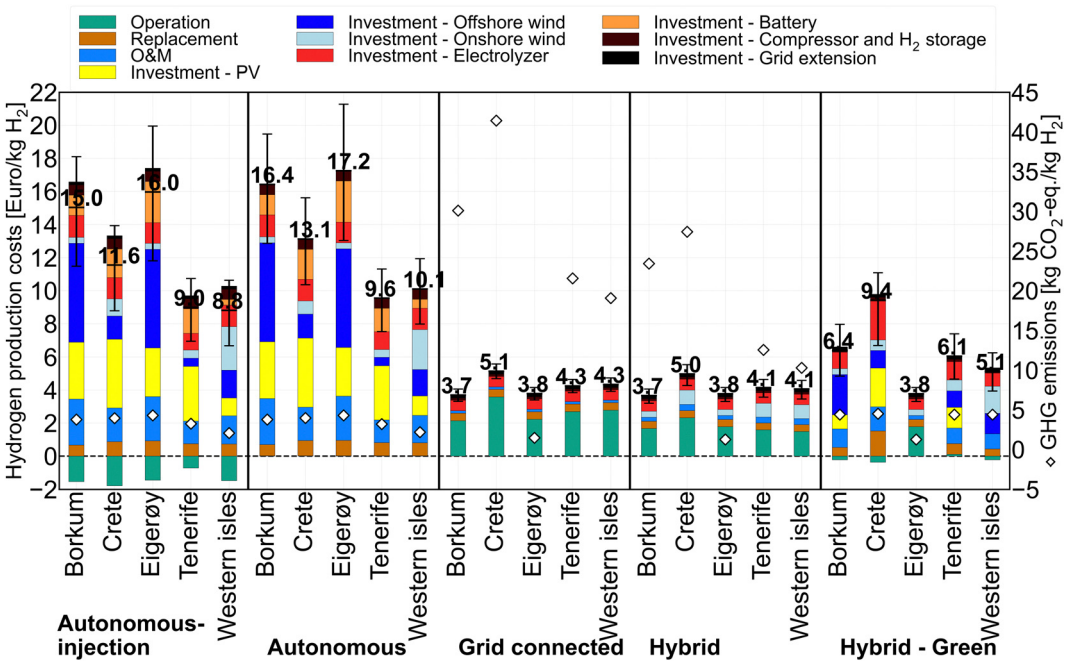

Fig. 4 Contribution analysis of hydrogen production costs [Euro per kg H_2]. The figure visualizes the contributions with different colors regarding the operation, investments, replacement as well as the fixed O&M costs. The costs and/or GHG emissions per MJ hydrogen production can be obtained by dividing the figures with the lower heating value of hydrogen (120 MJ kg^{-1}). Further, the error bars visualize a pessimistic scenario (highest H_2 costs) and optimistic scenario (lowest H_2 costs) for the current situation. These techno-economic scenarios are presented in Section E.2 of the ESI.† A table on annualized costs is provided in Section G.6 of the ESI.†

3.1 Economics

Fig. 4 visualizes the hydrogen production costs for all system configurations and five case studies. The size and colors of the bar segments show the contributions of the different cost components. The total hydrogen production costs are provided above the bars (in Euro per kg H_2). The secondary *y*-axis represents the impacts on climate change (in kg CO_2-eq. per kg H_2), indicated by the white diamond marker.

The figure shows that hydrogen production costs of around 3.7 Euro per kg H_2 are within reach nowadays in locations with low grid electricity costs (in Borkum) and for hybrid systems at locations with a large potential of wind energy and a high capacity factor of the renewables, for example on Borkum and Eigerøy (see Table 2). Hybrid systems exhibit the lowest hydrogen production costs (3.7–5.0 Euro per kg H_2) for the following reasons: (1) the electricity grid can be used for surplus electricity injection using feed-in tariffs to generate revenue; (2) the grid can be utilized as backup electricity supply to generate hydrogen with very low, or even negative, grid electricity prices (*e.g.*, in Germany); and (3) cost-efficient renewable energy sources can be optimally integrated without the need for additional (expensive) energy storage systems. These hybrid configurations can exhibit GHG emissions larger than the standards for green hydrogen (4.4 kg CO_2-eq. per kg H_2), see the secondary *y*-axis.[42] Alternatively, the hybrid-green configuration generates green hydrogen, although at higher hydrogen production costs between 3.8–9.4 Euro per kg H_2. Hydrogen production costs increase especially in countries with a GHG intensive grid electricity network (Germany and Greece). It is worth noting that the green hydrogen production standard cannot be reached in Crete with such a system configuration and therefore a GHG emission minimization is performed in this situation, reaching 4.5 kg CO_2-eq. per kg H_2. Nowadays, producing hydrogen, using water electrolysis, with low costs and low GHG emissions can only be achieved at very specific locations, such as Eigerøy and to a less extent in Western Isles.

Grid-connected systems perform well on overall costs when using "historical" day-ahead grid electricity prices (including grid fees). Grid electricity absorption is the main contributor to the overall hydrogen production costs. Lowest hydrogen production costs for grid-connected configurations are therefore obtained in countries with the lowest day-ahead grid electricity prices, for example in Borkum (Germany) with 3.7 Euro per kg H_2.

Hydrogen production costs for autonomous configurations are comparably high nowadays (9.6–17.2 Euro per kg H_2). This can be explained by the fact that there is a large capacity of renewable energy technologies installed, which requires a huge investment, to ensure a fully autonomous energy system operation, entirely disconnected from the electricity grid. For all autonomous configurations, the renewable electricity generators are oversized and a large amount of electricity generation is curtailed. Further, locations with constrained land availability (Borkum and Eigerøy) exhibit higher costs, since there is insufficient land available to install sufficient onshore wind and PV arrays, therefore additional offshore wind has to be installed with higher costs. In other words, larger geographical islands are preferred for large-scale hydrogen production systems to circumvent location-specific constraints regarding land occupation. Autonomous configurations with larger system components and most electricity curtailment logically perform worst, see also Table 3. Autonomous-grid injection configurations can slightly reduce net hydrogen production

Table 3 Installed capacity of energy technologies as well as curtailment of electricity (only for autonomous configurations) in the considered case studies as outcome of the optimization problem. CF = capacity factor, curt. = curtailment, cap. = capacity, Electr. = electrolyzer

Location [km^2 land]	Configuration	CF [-]	Electr. cap. [MW]	Wind cap. off [MW]	Wind cap. on [MW]	PV cap. [MW]	Battery energy cap. [MWh]	Battery power [MW]	Wind curt. off [%]	Wind curt. on [%]	PV curt. [%]
Crete	Grid connected	1.00	23								
[8450 km^2]	Hybrid	0.96	24		24						
	Hybrid-Green	0.26	86	15	18	95					
	Autonomous	0.48	47	21	22	170	329	80	34	36	61
	Autonomous - inj.	0.49	46	20	29	169	315	73	11	11	5
Eigerøy	Grid connected	1.00	23								
[20 km^2]	Hybrid	1.00	23		10						
	Hybrid-Green	1.00	23		10						
	Autonomous	0.51	45	85	10	120	500	41	71	38	50
	Autonomous - inj.	0.51	45	85	10	120	500	41	18	10	7
Western Isles	Grid connected	1.00	23								
[3070 km^2]	Hybrid	1.00	23		23						
	Hybrid-Green	0.80	29	18	45						
	Autonomous	0.49	47	23	66	48	101	19	52	54	45
	Autonomous - inj.	0.48	47	24	72	44	61	15	4	7	10
Tenerife	Grid connected	1.00	23								
[2030 km^2]	Hybrid	1.00	23		23						
	Hybrid-Green	0.57	40	14	18	51					
	Autonomous	0.60	38	7	13	133	266	50	19	19	42
	Autonomous - inj.	0.64	36	7	14	135	280	49	0	1	0
Borkum	Grid connected	1.00	23								
[30 km^2]	Hybrid	1.00	23		10						
	Hybrid-Green	0.64	36	35	10	35					
	Autonomous	0.48	48	86	10	140	231	35	68	64	71
	Autonomous - inj.	0.48	48	86	10	140	231	35	24	17	18

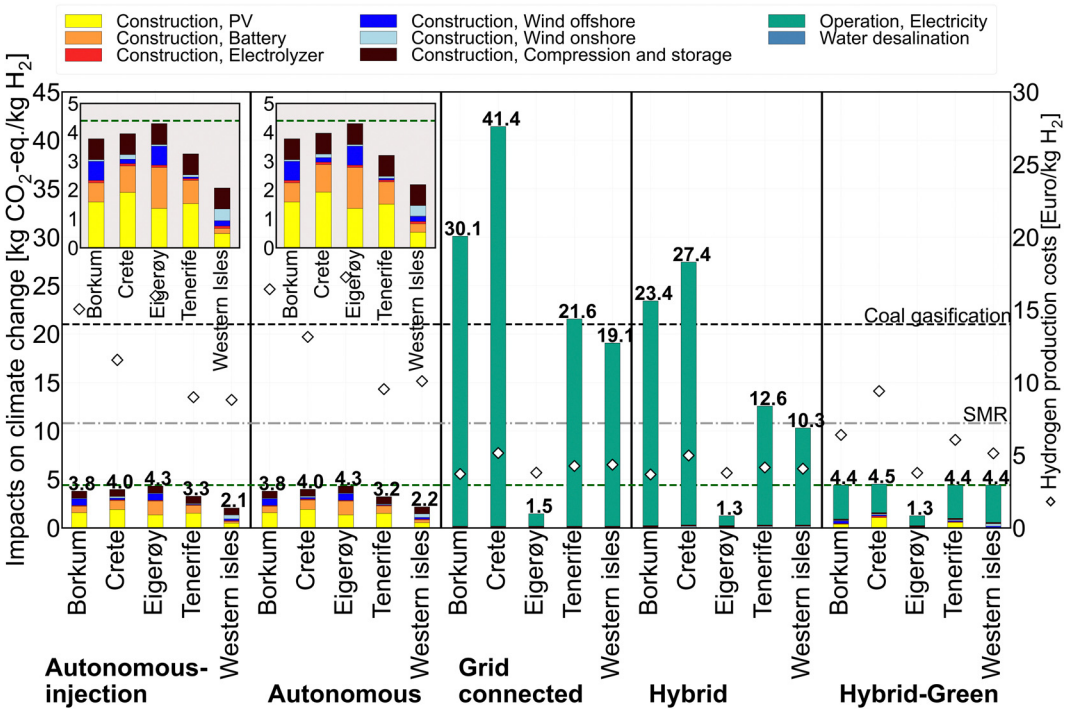

Fig. 5 Contribution analysis regarding life cycle GHG emissions of hydrogen production [kg CO_2-eq. per kg H_2]. The zoom (on the top left) of the figure provides more details for autonomous system configurations. The colored horizontal lines indicate the climate change impact of green hydrogen (green), gray hydrogen (in gray, dash-dotted) and black hydrogen (in black).[20] According to "CertifHy", renewable hydrogen should have a reduction of (at least) 60%—*i.e.*, lower than approximately 4.4 kg CO_2-eq. per kg H_2 (the dotted green line)—compared to hydrogen production *via* SMR of natural gas.[28,42]

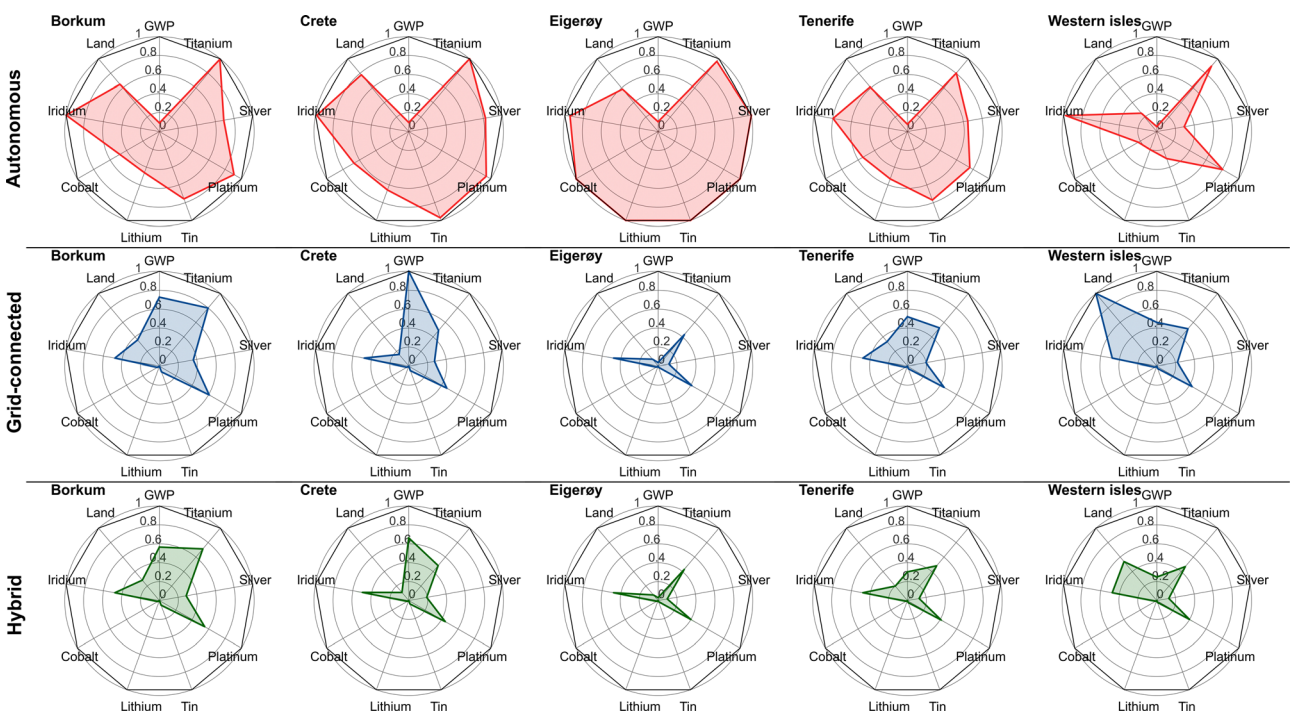

Fig. 6 Spider graphs for the selected system configurations and locations. The individual graphs illustrate the trade-offs regarding the selected environmental impact categories and resource utilization. Indicators are shown normalised in each case; "1" represents the respective maximum, for one of the considered configurations (hybrid, grid-connected, and autonomous). Red, blue, and green colors illustrate autonomous, grid-connected, and hybrid configurations, respectively. GWP = global warming potential (100a) equivalent to impacts on climate change.

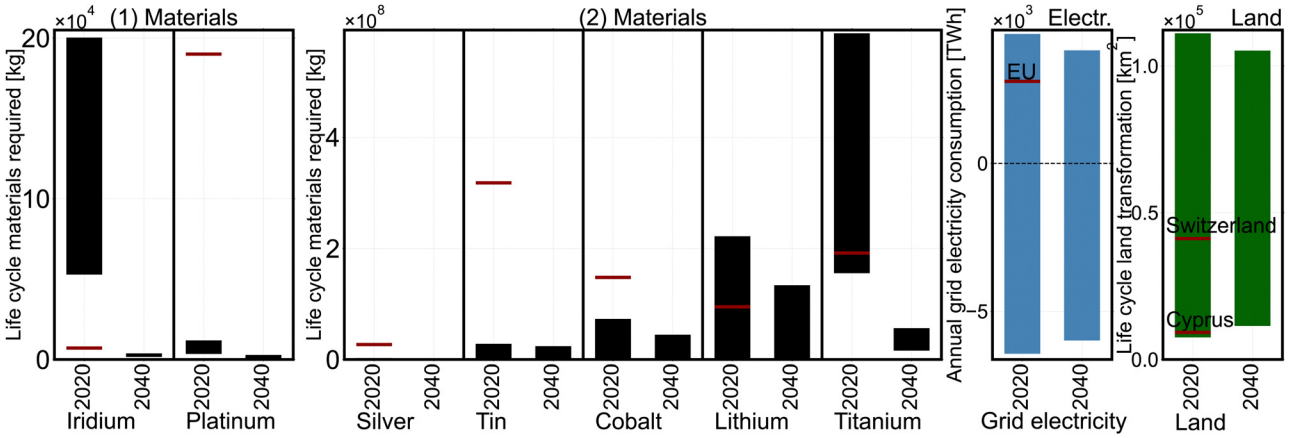

Fig. 7 This figure visualizes the minimum and maximum amount of materials, electricity, and land used in the hydrogen production configurations as assessed in our analysis. The reference magnitudes indicating annual production volumes and electricity generation[83] are valid for year 2018 and 2019 (instead of 2020), respectively.

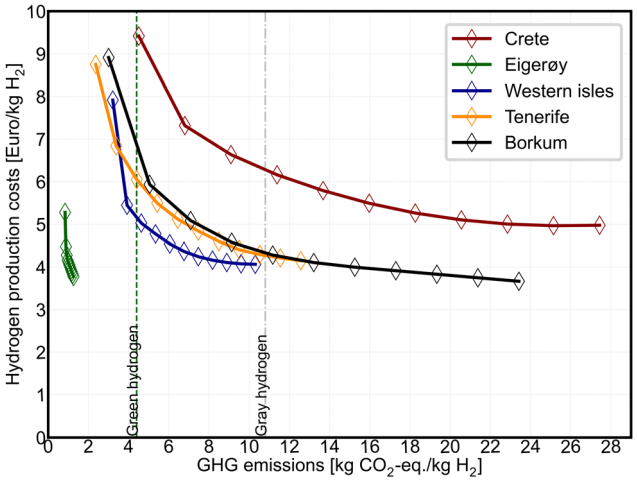

Fig. 8 Pareto fronts for hybrid configurations with life cycle GHG emissions on the *x*-axis and hydrogen production costs on the *y*-axis.

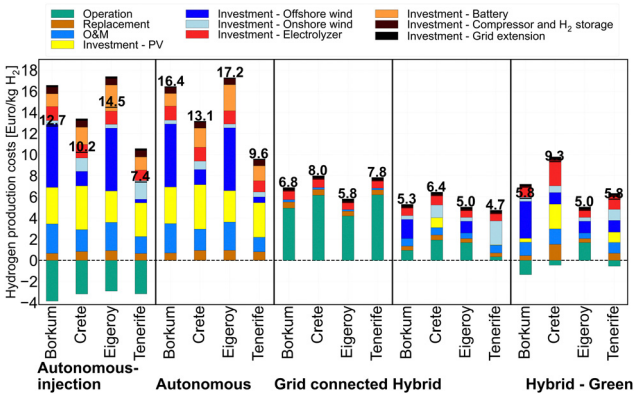

Fig. 9 Results from using the day-ahead electricity prices from year 2021. Grid electricity prices are not available for the entire year 2021 for the UK (Western Isles), we therefore exclude Western Isles for this exercise.

costs to 8.8–16.0 Euro per kg H_2, since revenue can be made from selling electricity to the electricity network using feed-in tariffs. Further, curtailment of excess (renewable) electricity is therefore significantly reduced and largely replaced for the injection into the electricity grid network, see Table 3 and Section G.5 of the ESI.†

These results imply that higher variability of renewable energy generation needs higher flexibility in terms of additional energy storage capacity installed, and/or requires additional capacity of renewable electricity generators, which most likely results in higher curtailment of renewable electricity. When there is more fluctuation of wind electricity generation, comparably high capacities of renewable energy generators and battery electricity storage are installed, for example in Eigerøy (where the maximum battery capacity is installed). In these situations, a larger battery is installed to store electricity to be used during time periods with low renewable electricity supply, to generate sufficient hydrogen during time periods with discontinued renewable electricity generation. It is worth noting that this is required to comply with the hydrogen production rate, which has been set as a constraint in our optimization problem. The annualized costs are therefore mainly dominated by investments in (renewable) energy technologies and the battery system in this situation, while the direct operation costs are very low or even negative (*i.e.*, revenue) for autonomous-grid injection configurations. In general, costs for water desalination (0.018 Euro per kg H_2) are relatively minor in comparison to the total hydrogen production costs.

3.2 Environmental analysis

3.2.1 Climate change impacts. Fig. 5 illustrates life cycle GHG emissions (in kg CO_2-eq. per kg H_2) of hydrogen production for each configuration. The different colors visualize the contributions of different processes needed for hydrogen production during the life cycle from cradle-to-gate. The zoom on the top left of the figure shows more details for autonomous configurations. For comparison, the horizontal lines in black, gray,[20] and green

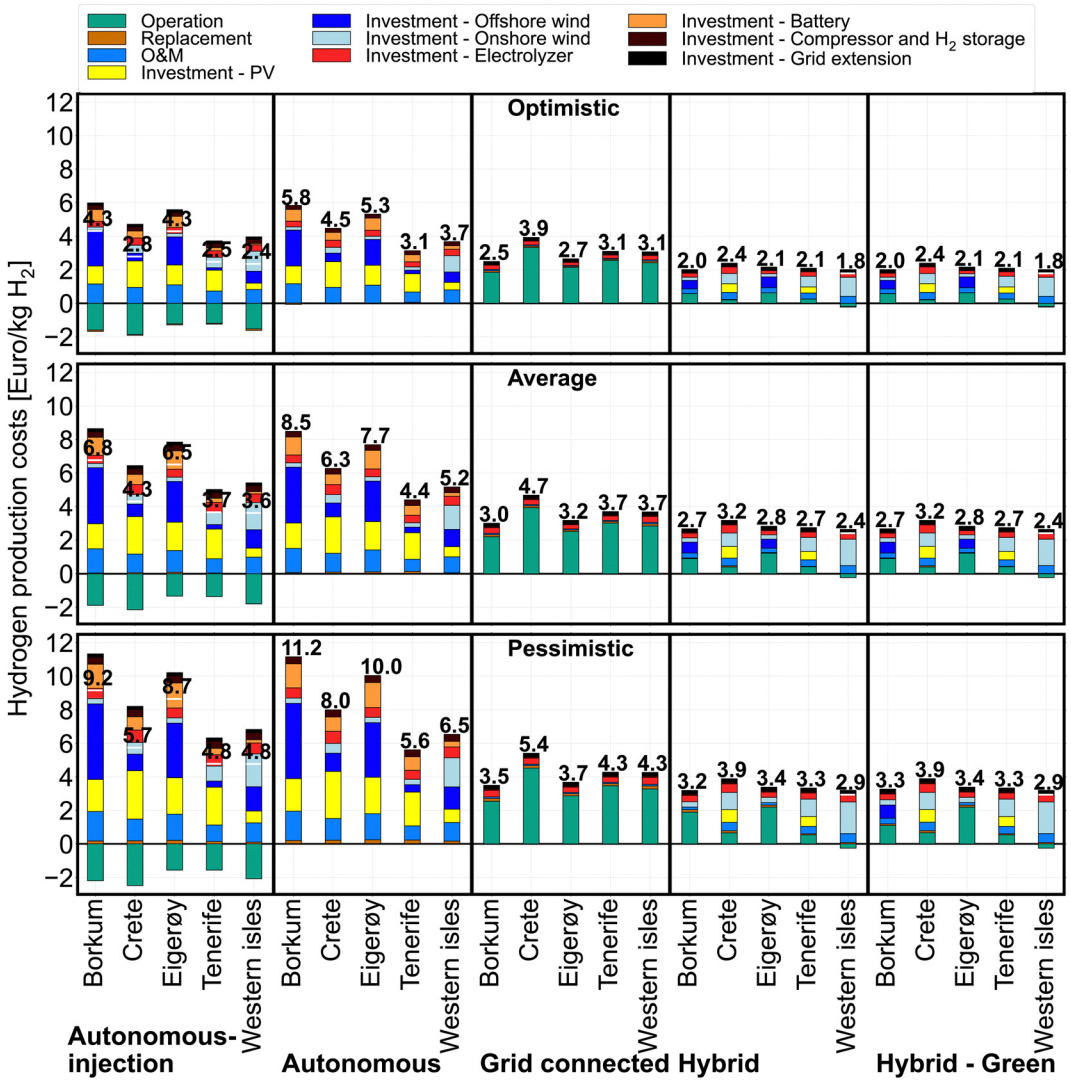

Fig. 10 A contribution analysis of future hydrogen production costs valid for year 2040 [Euro per kg H_2]. The figure visualizes the contributions with different colors regarding the operation, investments, replacement, and the fixed O&M costs.

visualize the climate change impacts of black (coal gasification), gray (SMR), and green hydrogen, respectively.[42]

Fig. 5 demonstrate that only autonomous configurations and a few other case studies exhibit GHG emissions below the threshold for green hydrogen as specified by Certifhy.[42] The GHG emissions of hydrogen production system configurations are mainly affected by: (1) the availability and continued supply of renewable electricity for configurations coupled to renewable electricity generators, and (2) the GHG intensity of the electricity grid for grid-coupled and hybrid configurations. The lowest GHG emissions (1.3 kg CO_2-eq. per kg H_2) are generated from the hybrid configuration in Eigerøy (Norway), since this configuration is coupled to a very low GHG intensive electricity grid in Norway.

Autonomous configurations exhibit low GHG emissions (2.1–4.3 kg CO_2-eq. per kg H_2) in general, since they are entirely based on wind and PV solar energy sources. However, the production of the larger (over)sized autonomous configurations—in terms of system components, including batteries—cannot be neglected, since they could exhibit climate change impacts approaching green hydrogen production thresholds. Autonomous configurations with large (onshore) wind availability exhibit the lowest GHG emissions with 2.1–2.2 kg CO_2-eq. per kg H_2 in Western Isles. Autonomous configurations which incorporate a large capacity of PV solar exhibit slightly higher GHG emissions of 3.2–4.3 kg CO_2-eq. per kg H_2. This can be mainly explained by the lower capacity factor of PV, in combination with the relatively GHG intensive production of PV wafers compared to wind turbine construction and the need for larger battery capacities.

The GHG emissions of grid-connected configurations mainly depend on the GHG intensity of the electricity grid, and are between 1.5 and 41.4 kg CO_2-eq. per kg H_2. From an environmental perspective, they only might be a sound option in countries with very low GHG intensive grid electricity and the option of expanding low-carbon generation capacities. Grid-connected configurations must therefore be avoided in

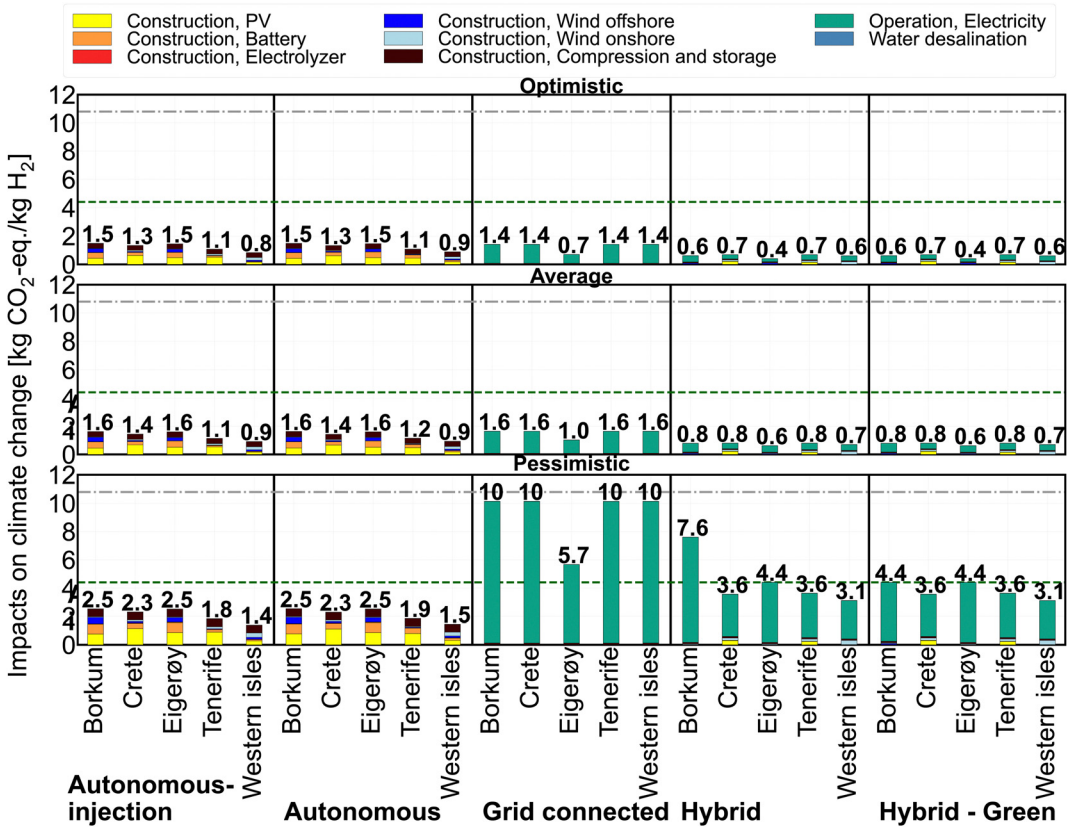

Fig. 11 A contribution analysis of future GHG emissions emitted from hydrogen production valid for year 2040 [kg CO_2-eq. per kg H_2] using The REgional Model of INvestments and Development (REMIND)[86,92] scenarios. Contributions from processes are visualized with different colors.

countries with a GHG intensive grid electricity mix, as for example in Greece and Germany, and in countries with constrained potentials for expansion of low-carbon generation. In the former case, hydrogen production exhibits (by far) larger GHG emissions than coal-based hydrogen production. This is also illustrated by Fig. A2 in Section G.1 of the ESI.†

Further, hybrid configurations are effective to reduce both annualized costs and GHG emissions, since they integrate locally available wind energy sources and therefore exhibit lower GHG emissions (1.3–27.4 kg CO_2-eq. per kg H_2) compared to grid-connected systems. However, configurations which absorb large amounts of GHG intensive grid electricity in a cost optimization—*e.g.*, in Crete (Greece) and Borkum (Germany)—still exhibit higher GHG emissions than gray and black hydrogen. The Pareto fronts of the hybrid configurations are shown in Section 3.3.1, to illustrate the optimization trade-offs between costs and GHG emissions. And lastly, the green hydrogen production standard can be reached by adding a constraint on the GHG emission objective, reaching low GHG emissions for all hybrid configurations for the Hybrid-Green alternative, although this exhibits (slightly) higher hydrogen production costs.

3.2.2 Impacts on (scarce) materials and land transformation. Fig. 6 illustrates environmental life cycle burdens for the 15 main configurations in terms of impacts on climate change, land transformation, and utilization of selected metals per kilogram hydrogen production. The spider graphs contain scores (from 0 to 1), normalized to the highest score for each indicator for the three main configurations (autonomous, grid-connected, and hybrid). Absolute results can be found in Section F of the ESI,† including the results for the sub-configurations. Further, Section G.3 in the ESI† provides a discussion and contribution analysis regarding land transformation.

Fig. 6 demonstrates that autonomous configurations lead to relatively high material utilization, due to larger system components installed, especially in Crete (Greece) and Eigerøy (Norway), where—compared to the other locations—renewable resources are less available or are constrained. The larger sized system components require an additional amount of materials, especially for the battery, renewable energy generators, and the electrolyzer. The impacts on climate change are, however, significantly smaller compared to most grid-connected configurations. Results of grid-connected configurations are mainly influenced by the grid electricity mix, with high indirect impacts on climate change for fossil fuel based grid electricity mixes. Hybrid configurations generally tend to exhibit the lowest environmental burdens for the selected indicators, visualized by the smaller colored area.

3.2.3 Scaling-up hydrogen production with PEM in 2040. Several hydrogen roadmaps predict that hydrogen can be a key element in the transition towards a net zero global energy system.[1,84] It is worth noting that hydrogen roadmaps depend

strongly on the future scenario chosen and can be developed on business as usual pathways (*i.e.*, current policies) as well as on preferred outcomes; for example a net zero global energy system.[85,86] These scenarios are usually based on integrated assessment models (IAMs). Sustainable and net zero pathways typically integrate hydrogen as essential energy vector in the total energy mix.[85,86] In our analysis, we adopt the figures provided in IRENA's REmap scenario for year 2050, with 19 EJ produced worldwide from renewable powered hydrogen.[84] Assuming a linear increase from 0 EJ in 2020 to 19 EJ in 2050, we reach 12.7 EJ in 2040. We further assume that 75% of this renewable hydrogen amount will be produced from PV and wind electrolysis in 2040 (*i.e.*, a total of 9.5 EJ is required). For this exercise, the 2040 scenario assumes the cost and technology specifications of the average scenario provided for year 2040 in Table 1, and therefore considers a modification of the foreground (see for these assumptions Section D of the ESI†) as well as background LCA database using the representative concentration pathway (RCP) 2.4 W m^{-2} IAM scenario only.

Fig. 7 illustrates cumulative annual, life cycle based utilization of (scarce) materials, land, and electricity for such an annual hydrogen production of 9.5 EJ considering all assessed configurations and case studies for two years (2020 and 2040). The range is based on the minimum (bottom of a bar) and maximum (top of a bar) impact considering all configurations based on a cost optimization. The selected materials include cobalt, iridium, lithium, platinum, silver, tin, and titanium. Current annual production volumes of all materials (except iridium), used as reference quantities to estimate potential scarcity coming along with up-scaling, are obtained from USGS for year 2018,[87] while the iridium production is obtained from Kiemel *et al.*;[88] these annual production volumes are provided for all materials with a red marker above, within, or below the bar segments. Therefore, an annual material requirement higher than the current annual production volume of a material implies that the large-scale implementation of hydrogen production with our system configurations might result in a shortage of material supply. Further, several reference magnitudes are provided, indicated with a red marker, for grid electricity and land transformation as well, such as the annual electricity generation in Europe (EU) and the total land area of Cyprus and Switzerland.

Materials. Fig. 7 shows that iridium will most likely be a scarce material on the short-term, when the large-scale deployment of water electrolysis is based on PEM electrolyzers. The configurations with the largest installed PEM electrolyzer capacity exhibit the highest material utilization for iridium, since iridium functions as catalyst in PEM electrolyzers. Titanium and lithium are other two materials, which (partially) cross the scarcity threshold. Titanium is mainly used for the bipolar plates in the stacks of the PEM electrolyzer, while lithium is mainly utilized in configurations with battery electricity storage for the NMC cathode. It is worth noting that expected technological improvements of iridium consumption indeed result in much lower iridium consumption,[88] thus most likely will not lead to shortages in the long-terms, this could, however, still be the case for lithium when a large battery is required.

On the one hand, the amount of material utilization can be (much) higher when installing the whole energy system in the first year, since the first installation of the energy system extracts most materials from the environment. On the other hand, most materials can be recycled after utilization and can be used in the next product cycle, which could significantly reduce material scarcity.[89] Further, material efficiency might reduce material scarcity in the coming years due to technological improvements, especially regarding iridium utilization in PEM electrolyzers.[50] Therefore, we included a future scenario for year 2040 using updated LCI for the battery and the electrolyzer, see Section D of the ESI,† for these assumptions.

Electricity. In addition, we examine grid electricity consumption when scaling up hydrogen production with PEM electrolyzers. The impact is indicated by the blue bars in Fig. 7, which demonstrates that the grid electricity requirement for PEM electrolyzers can be larger than the total European electricity generation in 2019. This implies a significant burden on the electricity grid network, especially when most hydrogen production will be installed as grid-connected configurations. It is worth mentioning that the scenario in year 2040 also shows a potential net electricity generation, due to the injection of excess PV and wind electricity generation into the electricity grid for some configurations.

Land. Further, the analysis regarding land transformation demonstrates that the maximum amount of land area requirement for the large-scale deployment of water electrolysis can be almost three times larger than the total land surface area of Switzerland, mainly due to indirect land transformation generated from grid electricity production as well as the large direct land area required for ground-mounted PV installations (see Section G.3 in the ESI†). This land area could not be available, and this could therefore limit the deployment of ground-mounted PV-coupled (considering a lifetime of 30 years) hydrogen production systems. On the contrary, the minimum land transformation obtained is $\sim$7500 km^2, and this is only 80% of the land surface area of Cyprus, or 6% of the land surface area of Greece.

3.3 Sensitivity analysis

3.3.1 Pareto: hybrid configurations. Fig. 8 shows the Pareto fronts for hybrid configurations with GHG emissions on the *x*-axis and hydrogen production costs on the *y*-axis. The locations are indicated with different colors. The markers in the top left of the plot represent a minimization on GHG emissions, while the markers in the bottom right of the plot represent a minimization on costs. The markers between these points consider both objectives. The climate change impact of green hydrogen is indicated by dashed green line, meaning that all Pareto points on the left of this graph meet the climate change impact requirements of green hydrogen production according to CertifHy.[42]

The figure demonstrates that hybrid configurations can significantly reduce costs and GHG emissions compared to grid-connected configurations. An optimization on annualized costs logically results in higher GHG emissions, however, these can be reduced when adding a constraint on life cycle GHG emissions. Locations with fossil fuel based grid connections are mostly influenced, manifested by the wider ranged Pareto front, for example in Greece. On the one hand, high GHG reductions of more than 80% can be achieved in Crete (Greece) approaching the carbon footprint of green hydrogen, even with a very high GHG intensive electricity grid in Greece. On the other hand, decarbonized electricity supply in Norway shows that only very minor GHG reductions can be achieved with hybrid configurations coupled to renewable energy generators in this situation. The latter figure also demonstrates that significant GHG emission reductions can be achieved for a small increase of hydrogen costs, especially in Crete and Borkum. It is worth mentioning that the overall costs of hydrogen in combination with a certain life cycle GHG reduction goal can be explored over the entire Pareto front, and a final decision can be made based on the preference of a system designer. One option is to run a cost optimization and to apply a constraint on the total GHG emissions to achieve green hydrogen production standards, as we performed with the ''Hybrid-Green'' configuration.

3.3.2 Increase of energy prices in 2021. Global energy prices increased significantly over year 2021. Electricity prices reached record levels in Europe with an average annual electricity price increase between 80–155% for the locations considered in this work.[90] We therefore assess the influence of increasing day-ahead electricity prices on hydrogen production costs, using the 2021 day-ahead electricity prices for the electricity market regions considered.

Fig. 9 illustrates the influence of higher grid electricity prices on the considered configurations for the different geographical islands. Fig. 9 is a bar plot showing the hydrogen production configurations on the *x*-axis and the score on the hydrogen production costs on the *y*-axis. The colored bar segments show the absolute contribution of different cost components to the overall hydrogen production costs. The total hydrogen production costs are provided above the bars.

It turns out that all configurations, except the fully autonomous configuration, are affected by an increase in electricity prices. Grid-connected systems become significantly more expensive with an increase from 3.7–5.1 Euro per kg H_2 to 5.8–8.0 Euro per kg H_2, since they entirely rely on grid electricity. Hybrid configurations become slightly more expensive, although the hydrogen price increase is smaller compared to grid-connected systems as they can (partly) replace grid electricity by installing (cheaper) renewable electricity sources. The autonomous-injection configuration benefits from higher grid electricity prices, since more revenue can be made by selling excess (renewable) electricity to the electricity network. Interestingly, green hydrogen production—especially the hybrid configurations—already achieves cost-parity with (grey) hydrogen production from natural gas steam reforming today, considering the recent price surge of natural gas leading to potential hydrogen production costs of 4–6 Euro per kg H_2 when using natural gas reforming.[91]

It is worth noting that large-scale hydrogen production operators could agree on long-terms grid electricity price contracts and therefore could prevent such a reliance on variable electricity prices. This might be a good option for the current energy price crises in Europe, especially for (fully) grid-connected hydrogen production systems.

3.3.3 Sensitivity to weather data inputs. Fig. A5 in Section G.4 of the ESI,† shows that especially the costs of hybrid configurations are hardly affected by different meteorological variabilities; this is visualized by the relatively small spread of the colored markers per location on the *y*-axis. In general, this implies that the calculated costs of hybrid configurations are reliable and do not differ significantly between the set of meteorological years.

The autonomous configurations exhibit, however, significant differences between meteorological years especially in terms of hydrogen production costs and to a lesser extent of GHG emissions. For example, the autonomous configuration can reach hydrogen production costs as low as 9 Euro per kg H_2 in Borkum, while other reference years reach hydrogen production costs up to 15 Euro per kg H_2. The optimal designs of the autonomous configurations are therefore significantly modified depending on these different weather conditions in each meteorological year. Comparing the different case studies suggests that locations with high shares of solar PV supply, due to high solar yields (Tenerife and Crete), are subject to less variability than these primarily supplied by wind power. Further, it is worth noting that missing data or outages of energy generators most likely result in larger energy system components, especially for autonomous configurations. In this situation, additional storage capacity or renewable energy capacity (with curtailment) is integrated to overcome the discontinuation of renewable energy generation. In reality, other solutions can be proposed, such as planned outages instead of assuming a stable hydrogen production output as assumed in this work. In general, the optimal designs of autonomous configurations are more sensitive to changes in (annual) weather conditions and outages as there is no electricity grid for backup supply. In other words, the optimal designs of the autonomous configurations are less robust compared to the hybrid and grid-connected configurations.

This implies that more attention should be given for the optimal design of autonomous energy systems. For example, the optimal design could be based on a larger set of design years to generate the meteorological design year. Further, a comprehensive sensitivity analysis as well as a robustness analysis could be used to provide more reliable insights.

3.3.4 Future situation in 2040. Fig. 10 shows a contribution analysis of (possible) future hydrogen production costs for all considered case studies using optimistic, average, and pessimistic cost scenarios. The associated cost numbers and technology specifications for these scenario are provided in Table 1. Further, assumptions regarding grid electricity are provided in Table 4. Again, the colors illustrate different cost

Table 4 Assumed electricity prices as well as the GHG intensity of the electricity grid for year 2040

Location		Pessimistic (2040)		Average (2040)		Optimistic (2040)	
		Price [Euro per kWh]	GHG intensity [kg CO_2-eq. per kWh]	Price [Euro per kWh]	GHG intensity [kg CO_2-eq. per kWh]	Price [Euro per kWh]	GHG intensity [kg CO_2-eq. per kWh]
Crete	Greece	0.095	0.208	0.083	0.032	0.071	0.028
Eigerøy	Norway	0.058	0.115	0.051	0.020	0.043	0.013
Western Isles	United Kingdom	0.073	0.208	0.064	0.032	0.054	0.028
Tenerife	Spain	0.071	0.208	0.062	0.032	0.053	0.028
Borkum	Germany	0.056	0.208	0.049	0.032	0.042	0.028

components, and the total hydrogen costs are presented above the bars.

Fig. 10 shows that future hydrogen production costs of approximately 2–3 Euro per kg H_2 are within reach for hybrid configurations in countries with a large availability of wind energy supply for the optimistic and average cost scenario; approaching cost parity with fossil fuel based hydrogen production pathways. The reduction of annualized costs can be mainly explained by the assumed reduction of investments in combination with extended lifetimes of system components. The cost of autonomous configurations is also significantly lower than today for all cost scenarios with hydrogen production costs varying between 2–11 Euro per kg H_2.

Fig. 11 illustrates prospective life cycle GHG emissions for all considered case studies with colors representing the different system components and their associated life cycle GHG emissions. The total GHG emissions per kg hydrogen production are provided above the bar segments. The assumptions for this prospective LCA are provided in Section D.1 of the ESI.† The latter figure demonstrates GHG emissions below 2 kg CO_2-eq. per kg H_2 for all hydrogen production configurations in the optimistic and average future scenario. The pessimistic scenario represents a business as usual scenario with less decarbonized grid electricity supply, and this therefore results in higher life cycle GHG emissions—up to more than 10 kg CO_2-eq. per kg H_2—for grid-connected configurations in particular.

4 Discussion

Several other important factors should be considered for the interpretation of our results and these are discussed in the following paragraphs. Further, limitations of our analysis and issues to be considered for future work are identified.

Some potentially important local boundary conditions were not considered in our analysis. For example, renewable power generation at a certain location can be limited by a maximum land area available for PV panels and/or wind turbines. We considered this in a generic way by limiting the maximum installed capacity for onshore wind turbines and PV systems. Further specific analysis regarding wind and PV potentials in terms of available land are required. Besides, the inclusion of grid capacity costs was simplified in our analysis, but should be addressed on a local level since these costs and regulations are very location-specific. The development of an entire grid electricity network from scratch—a ''greenfield'' approach—should be considered on geographical locations without a supply infrastructure, which inevitably exhibits additional costs and environmental burdens for grid-connected systems. Further, social factors can limit the deployment of renewable energy technologies.[93–95] Thus, besides economic, environmental, and technological factors analyzed in this work, socio-cultural and institutional factors should be considered when determining suitable locations for the development of large-scale hydrogen production facilities.

In addition, our system boundaries considered a cradle-to-gate approach to provide hydrogen at 80 bar pressure. However, the inclusion of further processing and transportation of hydrogen inevitably causes additional costs and environmental burdens, which must be addressed when the specific use case of hydrogen is known.[96,97]

This paper focused on environmental impacts regarding GHG emissions, land transformation, and material utilization. However, other environmental impact categories can be of importance as well. Water quality might be another important environmental concern, for example when a significant amount of brine—a co-produced high saline waste generated from desalination—is discharged into the marine environment.[57,98] In the context of water consumption, the large-scale deployment of hydrogen production in combination with expected additional water demand due to climate change, population growth, economic development, and agricultural intensification might result in water scarcity, which is already the case for Crete and Tenerife.[99,100] Such water scarcity assessments should be addressed on a regional level in future work.[101–103]

Further, technological material improvements—such as increased material efficiency as well as novel and alternative materials and systems[104–106]—in PEM electrolyzers could reduce material availability issues associated to the upscaling of hydrogen production with PEM electrolyzers. We considered this improved material efficiency using updated (future) foreground LCI of PEM electrolyzers in a simplified way,[50] and showed that improved material efficiency could significantly reduce material scarcity. To achieve this, current research is targeting alternative and lower cost materials—especially for the catalysts and membranes used[105]—to reduce (critical) material utilization.[14,104] Further, hydrogen leakage must be minimized to prevent undesirable radiative forcing, as hydrogen is an indirect greenhouse gas.[107] Such developments are of critical importance to enable a smooth transition towards the large-scale deployment of hydrogen production.

And lastly, we focused on the optimal design of large-scale hydrogen production system using a broad, though limited, set of technologies and geographical locations. This technology portfolio could be expanded by considering alternative batteries, electrolyzers, and hydrogen storage options in other favorable geographical locations. Other favorable geographical locations for large-scale hydrogen production exhibit high solar PV and/or wind potentials as well as land availability and easy access to a hydrogen transportation network (*e.g.*, over water). The global map in Section H of the ESI,† indicates that, for example, North-West Africa (Morocco), South-West of Australia, and the South-East of South-America exhibit such potentials. Further assessments are required to evaluate other potentially favorable hydrogen production locations on the mainland, especially in the United States and the North of Africa.

5 Conclusions

This paper quantified current and future hydrogen production costs as well as life cycle environmental burdens of large-scale hydrogen production *via* water electrolysis, with a focus on potentially favorable hydrogen production locations on geographical islands. Autonomous systems exclusively supplied by wind and/or PV power, grid-connected, and hybrid systems were analyzed.

Our results demonstrated that the amount of electricity consumed, its source and price, the (firm) supply of PV and wind electricity, and investments for system components are the most crucial factors for the overall costs and environmental burdens of large-scale hydrogen production configurations. Hydrogen production costs of 3.7 Euro per kg H_2 are within reach today for hybrid systems at favorable locations.

Future hydrogen production costs of hybrid systems might be reduced to approximately 2 Euro per kg H_2 in 2040—approaching cost parity with hydrogen from natural gas reforming when applying "historical" natural gas prices. The current rise of natural gas prices, however, represents a massive opportunity for green hydrogen production, since cost parity between grey and green hydrogen can already be achieved today.

Producing hydrogen by water electrolysis with low costs and low GHG emissions is only possible at very specific locations nowadays, such locations have a high availability and stable supply of renewable energy sources and sufficient land available. The lowest GHG emissions were achieved with hybrid configurations using a very low GHG intensive electricity grid in combination with wind power. Hybrid configurations could, however, exhibit substantial GHG emissions when supplied by GHG intensive electricity grids. Autonomous configurations, only supplied by renewables, exhibited low GHG emissions but comparatively high costs. The need for oversized system components and substantial electricity storage cannot be neglected. When it comes to the implementation of a hydrogen economy at large scale with substantial electrolysis capacities, it must be ensured that grid-connected configurations are only installed in parallel with sufficient amounts of additional low-carbon power generation.

Importantly, land use and material demand can represent limiting factors for a quick large-scale deployment of hydrogen production *via* water electrolysis. Especially iridium, needed for PEM electrolyzers, might be a scarce material in the short-term. Further, autonomous configurations with ground-mounted PV installations could require extensive land transformation. And lastly, the scale-up of hydrogen production might require substantial extensions of electricity grid networks when most hydrogen production plants are grid-connected.

Our findings imply that it is of great importance to substantially improve material efficiency of PEM electrolyzers as well as to consider complementary hydrogen production systems, for example from biomass,[31,108,109] to avoid potentially excessive costs of for example scarce materials. Especially the electrolyzer industry must improve economically, before green hydrogen can be considered as a cost-effective decarbonization option. We demonstrated that a substantial reduction of overall costs and environmental burdens can be achieved with optimal planning, siting, and sizing of green hydrogen production facilities. When these prerequisites are met, cost competitive hydrogen production *via* water electrolysis is within reach and can contribute to a low-carbon global energy system.

Author contributions

Tom Terlouw: Conceptualization, software, methodology, formal analysis, visualization, writing—original draft. Christian Bauer: conceptualization, supervision, writing—review & editing. Russell McKenna: supervision, writing—review & editing. Marco Mazzotti: supervision, writing—review & editing.

Conflicts of interest

There are no conflicts to declare.

Acknowledgements

The authors thank Idar Sønstabø (Dalane Energi, Norway) and other colleagues involved in the ROBINSON project for data provision. The authors further thank Romain Sacchi (PSI, Switzerland) for the provision of updated LCIs regarding PV systems. And lastly, the authors thank Evangelos Panos (PSI) for his insights on the economic analysis. This work has received funding from the European Union's Horizon 2020 Research and Innovation Programme under Grant Agreement N. 957752. Further financial support has been provided by the Swiss Federal Office of Energy (SFOE) *via* the research project "SHELTERED" and the Swiss ETH domain *via* the funds for "Coordinated Research", which allowed setting up of the Energy System Integration (ESI) Platform at PSI.

References

1 IEA, *Net Zero by 2050 - A Roadmap for the Global Energy Sector*, Iea technical report, 2021.

2 International Energy Agency, *The Future of Hydrogen*, International Energy Agency technical report, 2019.
3 European Commission, *A hydrogen strategy for a climate-neutral Europe [COM(2020) 301 final]*, European Commission technical report, 2020.
4 Office of Fossil Energy, *Hydrogen Strategy: Enabling A Low-Carbon Economy*, Department of Energy technical report, 2020.
5 IRENA, *Green Hydrogen Cost Reduction: Scaling up Electrolysers to Meet the 1.5 C Climate Goal*, IRENA technical report, 2020.
6 S. E. Hosseini and M. A. Wahid, *Renewable Sustainable Energy Rev.*, 2016, **57**, 850–866.
7 J. Rissman, C. Bataille, E. Masanet, N. Aden, W. R. Morrow III, N. Zhou, N. Elliott, R. Dell, N. Heeren and B. Huckestein, *et al.*, *Appl. Energy*, 2020, **266**, 114848.
8 C. Bauer, T. Heck, S. Schneider, H. Sanjaykumar, T. Terlouw, K. Treyer and X. Zhang, *Electricity storage and hydrogen: Technologies, costs and environmental burdens*, PSI, Paul Scherrer Institut technical report, 2021.
9 R. Bhandari, C. A. Trudewind and P. Zapp, *J. Cleaner Prod.*, 2014, **85**, 151–163.
10 R. Hanke-Rauschenbach, B. Bensmann and P. Millet, *Compendium of hydrogen energy*, Elsevier, 2015, pp. 179–224.
11 T. Nguyen, Z. Abdin, T. Holm and W. Mérida, *Energy Convers. Manage.*, 2019, **200**, 112108.
12 M. Carmo, D. L. Fritz, J. Mergel and D. Stolten, *Int. J. Hydrogen Energy*, 2013, **38**, 4901–4934.
13 M. Wang, Z. Wang, X. Gong and Z. Guo, *Renewable Sustainable Energy Rev.*, 2014, **29**, 573–588.
14 S. S. Kumar and V. Himabindu, *Mater. Sci. Energy Technol.*, 2019, **2**, 442–454.
15 A. Christensen, *International Council on Clean Transportation*, Washington, DC, USA, 2020, pp. 1–73.
16 M. Kayfeci, A. Keçebas and M. Bayat, *Solar hydrogen production*, Elsevier, 2019, pp. 45–83.
17 O. Schmidt, A. Gambhir, I. Staffell, A. Hawkes, J. Nelson and S. Few, *Int. J. Hydrogen Energy*, 2017, **42**, 30470–30492.
18 M. R. Shaner, H. A. Atwater, N. S. Lewis and E. W. McFarland, *Energy Environ. Sci.*, 2016, **9**, 2354–2371.
19 B. Parkinson, P. Balcombe, J. Speirs, A. Hawkes and K. Hellgardt, *Energy Environ. Sci.*, 2019, **12**, 19–40.
20 T. Longden, F. J. Beck, F. Jotzo, R. Andrews and M. Prasad, *Appl. Energy*, 2021, **266**, 118145.
21 S. Hellweg and L. Milà i Canals, *Science*, 2014, **344**, 1109–1113.
22 T. Terlouw, C. Bauer, L. Rosa and M. Mazzotti, *Energy Environ. Sci.*, 2021, **14**, 1701–1721.
23 M. Voldsund, K. Jordal and R. Anantharaman, *Int. J. Hydrogen Energy*, 2016, **41**, 4969–4992.
24 C. Bauer, K. Treyer, C. Antonini, J. Bergerson, M. Gazzani, E. Gencer, J. Gibbins, M. Mazzotti, S. T. McCoy, R. McKenna, R. Pietzcker, A. P. Ravikumar, M. C. Romano, F. Ueckerdt, J. Vente and M. van der Spek, *Sustainable Energy Fuels*, 2022, **6**(1), 66–75.
25 R. W. Howarth and M. Z. Jacobson, *Energy Sci. Eng.*, 2021, 1676–1687.
26 M. C. Romano, C. Antonini, A. Bardow, V. Bertsch, N. P. Brandon, J. Brouwer, S. Campanari, L. Crema, P. E. Dodds and S. Gardarsdottir, *et al.*, *Energy Sci. Eng.*, 2022, **10**(7), 1944–1954.
27 R. W. Howarth and M. Z. Jacobson, How green is blue hydrogen?, *Energy Sci. Eng.*, 2022, **9**(10), 1676–1687.
28 G. Palmer, A. Roberts, A. Hoadley, R. Dargaville and D. Honnery, *Energy Environ. Sci.*, 2021, **14**, 5113–5131.
29 E. Cetinkaya, I. Dincer and G. Naterer, *Int. J. Hydrogen Energy*, 2012, **37**, 2071–2080.
30 A. Al-Qahtani, B. Parkinson, K. Hellgardt, N. Shah and G. Guillen-Gosalbez, *Appl. Energy*, 2021, **281**, 115958.
31 C. Antonini, K. Treyer, A. Streb, M. van der Spek, C. Bauer and M. Mazzotti, *Sustainable Energy Fuels*, 2020, **4**, 2967–2986.
32 D. S. Mallapragada, E. Gençer, P. Insinger, D. W. Keith and F. M. OSullivan, *Cell Rep. Phys. Sci.*, 2020, **1**, 100174.
33 P. Marocco, D. Ferrero, M. Gandiglio, M. Ortiz, K. Sundseth, A. Lanzini and M. Santarelli, *Energy Convers. Manage.*, 2020, **211**, 112768.
34 P. Marocco, D. Ferrero, E. Martelli, M. Santarelli and A. Lanzini, *Energy Convers. Manage.*, 2021, **245**, 114564.
35 F. V. Matera, C. Sapienza, L. Andaloro, G. Dispensa, M. Ferraro and V. Antonucci, *Int. J. Hydrogen Energy*, 2009, **34**, 7009–7014.
36 T. Terlouw, X. Zhang, C. Bauer and T. Alskaif, *J. Cleaner Prod.*, 2019, **221**, 667–677.
37 International Energy Agency, *The Role of Critical Minerals in Clean Energy Transitions*, International Energy Agency technical report, 2021.
38 G. Notton, M.-L. Nivet, C. Voyant, C. Paoli, C. Darras, F. Motte and A. Fouilloy, *Renewable Sustainable Energy Rev.*, 2018, **87**, 96–105.
39 J. Bistline, *Environ. Sci. Technol.*, 2021, **55**, 5629–5635.
40 R. Sacchi, T. Terlouw, K. Siala, A. Dirnaichner, C. Bauer, B. Cox, C. Mutel, V. Daioglou and G. Luderer, *Renewable Sustainable Energy Rev.*, 2022, **160**, 112311.
41 Fraunhofer, *Photovoltaics Report*, 2021, **https://www.ise.fraunhofer.de/content/dam/ise/de/documents/publications/studies/Photovoltaics-Report.pdf**.
42 CertifHy, *CertifHy - Developing a European Framework for the generation of guarantees of origin for green hydrogen*, 2016, **https://www.certifhy.eu/images/media/files/CertifHy_-_definition_outcome_and_scope_LCA_analysis.pdf**, Accessed on Tuesday, September 31, 2021.
43 L. Bird, D. Lew, M. Milligan, E. M. Carlini, A. Estanqueiro, D. Flynn, E. Gomez-Lazaro, H. Holttinen, N. Menemenlis and A. Orths, *et al.*, *Renewable Sustainable Energy Rev.*, 2016, **65**, 577–586.
44 T. S. Schmidt, M. Beuse, X. Zhang, B. Steffen, S. F. Schneider, A. Pena-Bello, C. Bauer and D. Parra, *Environ. Sci. Technol.*, 2019, **53**, 3379–3390.
45 T. Terlouw, T. AlSkaif, C. Bauer and W. van Sark, *Appl. Energy*, 2019, **239**, 356–372.
46 PIK, *Price of Hydrogen: CAPEX Data*, 2021, **https://h2foroveralls.shinyapps.io/H2Dash/**.

47 R. Wiser, J. Rand, J. Seel, P. Beiter, E. Baker, E. Lantz and P. Gilman, *Nat. Energy*, 2021, **6**, 555–565.
48 BFE, *Photovoltaikmarkt- Beobachtungsstudie 2019*, Energieschweiz, bundesamt für energie bfe technical report, 2020.
49 M. S. Ziegler and J. E. Trancik, *Energy Environ. Sci.*, 2021, **14**, 1635–1651.
50 K. Bareiß, C. de la Rua, M. Möckl and T. Hamacher, *Appl. Energy*, 2019, **237**, 862–872.
51 L. Herenčić, M. Melnjak, T. Capuder, I. Andročec and I. Rajšl, *Energy Convers. Manage.*, 2021, **236**, 114064.
52 M. Minutillo, A. Perna, A. Forcina, S. Di Micco and E. Jannelli, *Int. J. Hydrogen Energy*, 2021, **46**, 13667–13677.
53 M. Beuse, B. Steffen and T. S. Schmidt, *Joule*, 2020, **4**, 2162–2184.
54 I. Petkov and P. Gabrielli, *Appl. Energy*, 2020, **274**, 115197.
55 D. Parra and M. K. Patel, *Int. J. Hydrogen Energy*, 2016, **41**, 3748–3761.
56 J. Yates, R. Daiyan, R. Patterson, R. Egan, R. Amal, A. Ho-Baille and N. L. Chang, *Cell Rep. Phys. Sci.*, 2020, **1**, 100209.
57 M. A. Khan, T. A. Al-Attas, S. Roy, M. Rahman, N. Ghaffour, V. Thangadurai, S. Larter, J. Hu, P. Ajayan and M. Kibria, *Energy Environ. Sci.*, 2021, **14**, 4831–4839.
58 Eurostat, *Household energy prices in the EU increased compared with 2018*, 2020, **https://ec.europa.eu/eurostat/databrowser/view/nrg_pc_204/default/table?lang=en**.
59 R. Baldick, *Applied optimization: Formulation and algorithms for engineering systems*, Cambridge University Press, 2006, vol. 9780521855, pp. 1–768.
60 T. Terlouw, T. AlSkaif, C. Bauer and W. van Sark, *Appl. Energy*, 2019, **254**, 113580.
61 C. Klemm and P. Vennemann, *Renewable Sustainable Energy Rev.*, 2021, **135**, 110206.
62 P. Gabrielli, M. Gazzani, E. Martelli and M. Mazzotti, *Appl. Energy*, 2018, **219**, 408–424.
63 P. Gabrielli, M. Gazzani and M. Mazzotti, *Appl. Energy*, 2018, **221**, 557–575.
64 B. Steffen, *Energy Economics*, 2020, **88**, 104783.
65 T. Huld, R. Müller and A. Gambardella, *Sol. Energy*, 2012, **86**, 1803–1815.
66 W. Holmgren, Calama-Consulting, C. Hansen, K. Anderson, M. Mikofski, A. Lorenzo, U. Krien, bmu, C. Stark, DaCoEx, A. Driesse, A. R. Jensen, M. S. de León Peque, konstant_t, mayudong, Heliolytics E. Miller, M. A. Anoma, V. Guo, L. Boeman, J. Stein, W. Vining, jforbess, T. Lunel, A. Morgan, J. Ranalli, C. Leroy, A. M. R. JPalakapillyKWH and J. Dollinger, *pvlib/pvlib-python: v0.9.0, Zenodo*, 2021, DOI: **10.5281/zenodo.5366883**.
67 W. F. Holmgren, C. W. Hansen and M. A. Mikofski, *J. Open Source Software*, 2018, **3**, 884.
68 S. Haas, U. Krien, B. Schachler, S. Bot, kyri petrou, V. Zeli, K. Shivam and S. Bosch, *wind-python/windpowerlib: Silent Improvements*, 2021.
69 Meteostat, *Meteostat Python Package*, 2021, **https://github.com/meteostat/meteostat-python**.
70 ENTSOE, *ENTSO-E Transparency Platform*, 2021, **https://transparency.entsoe.eu/dashboard/show**.
71 *Ecoinvent, ecoinvent 3.7.1.*, 2021, **https://ecoinvent.org/the-ecoinvent-database/data-releases/ecoinvent-3-7-1/**, Accessed on Sunday, October 31, 2021.
72 ISO, *ISO 14040: Life Cycle Assessment, Principles and Framework*, 2006.
73 ISO, *ISO 14044: Life cycle assessment - Requirements and guidelines*, 2006.
74 C. Mutel, *J. Open Source Software*, 2017, **2**, 236.
75 G. Wernet, C. Bauer, B. Steubing, J. Reinhard, E. Moreno-Ruiz and B. Weidema, *Int. J. Life Cycle Assess.*, 2016, **21**, 1218–1230.
76 R. R. Beswick, A. M. Oliveira and Y. Yan, *ACS Energy Lett.*, 2021, **6**, 3167–3169.
77 R. Frischknecht, P. Stolz, L. Krebs, M. de Wild-Scholten, P. Sinha, V. Fthenakis, H. C. Kim, M. Raugei and M. Stucki, *Life Cycle Inventories and Life Cycle Assessment of Photovoltaic Systems, International Energy Agency (IEA) PVPS Task 12, Report T12-19:2020*, 2020.
78 N. Brinkel, W. Schram, T. AlSkaif, I. Lampropoulos and W. Van Sark, *Appl. Energy*, 2020, **276**, 115285.
79 ROBINSON, *ROBINSON*, 2021, **https://www.robinson-h2020.eu/**.
80 European Union, *Communication from the commission to the european parliament, the european council, the council, the european economic and social committee and the committee of the regions*, European Union technical report, 2019.
81 European Union, *A strategic long-term vision for a prosperous, modern, competitive and climate-neutral EU economy*, European union technical report, 2019.
82 European Commission, *Hydrogen*, 2022, **https://energy.ec.europa.eu/topics/energy-system-integration/hydrogen_en**, Accessed on Tu, May 31, 2022.
83 Eurostat, *Electricity production, consumption and market overview*, 2021, **https://ec.europa.eu/eurostat/statistics-explained/index.php?title=Electricity_production,_consumption_and_market_overview**.
84 IRENA, *Hydrogen, A renewable energy perspective*, Irena, abu dhabi technical report, 2019.
85 A. Gambhir, J. Rogelj, G. Luderer, S. Few and T. Napp, *Energy Strategy Rev.*, 2019, **23**, 69–80.
86 E. Kriegler, N. Bauer, A. Popp, F. Humpenöder, M. Leimbach, J. Strefler, L. Baumstark, B. L. Bodirsky, J. Hilaire, D. Klein, I. Mouratiadou, I. Weindl, C. Bertram, J.-P. Dietrich, G. Luderer, M. Pehl, R. Pietzcker and F. Piontek, *et al.*, *Glob. Environ. Change*, 2016, **42**, 297–315.
87 USGS, *USGS Online Publications Directory*, 2021, **https://pubs.usgs.gov/periodicals/mcs2020/**.
88 S. Kiemel, T. Smolinka, F. Lehner, J. Full, A. Sauer and R. Miehe, *Int. J. Energy Res.*, 2021, **45**, 9914–9935.
89 C. Minke, M. Suermann, B. Bensmann and R. Hanke-Rauschenbach, *Int. J. Hydrogen Energy*, 2021, **46**, 23581–23590.

90 Bloomberg, *Europes Never Paid So Much for Power as 2021 Breaks Record, 2021*, **https://www.bloomberg.com/news/articles/2021-12-30/europe-has-never-paid-so-much-for-power-as-2021-costs-hit-record**, Accessed on Thursday, January 13, 2022.
91 G. Hieminga and N. Tillier, *High gas prices triple the cost of hydrogen production*, 2021, **https://think.ing.com/articles/hold-1of4-high-gas-prices-triples-the-cost-of-hydrogen-production**, Accessed on Tuesday, March 22, 2022.
92 G. Luderer, M. Leimbach, N. Bauer, E. Kriegler, L. Baumstark, C. Bertram, A. Giannousakis, J. Hilaire, D. Klein, A. Levesque, I. Mouratiadou, M. Pehl, R. Pietzcker, F. Piontek, N. Roming, A. Schultes, V. J. Schwanitz and J. Strefler, *Description of the REMIND model (Version 1.6)*, 2015, **https://ssrn.com/abstract=2697070**, Accessed on Thu, March 11, 2021.
93 M. Vasstrøm and H. K. Lysgård, *Energy Res. Soc. Sci.*, 2021, 102089.
94 S. Sen and S. Ganguly, *Opportunities, barriers and issues with renewable energy development - A discussion*, 2017.
95 R. McKenna, S. Pfenninger, H. Heinrichs, J. Schmidt, I. Staffell, C. Bauer, K. Gruber, A. N. Hahmann, M. Jansen and M. Klingler, *et al.*, *Renewable Energy*, 2022, **182**, 659–684.
96 M. van der Spek, C. Banet, C. Bauer, P. Gabrielli, W. Goldthorpe, M. Mazzotti, S. T. Munkejord, N. A. Røkke, N. Shah and N. Sunny, *et al.*, *Energy Environ. Sci.*, 2022, **15**, 1034–1077.
97 International Renewable Energy Agency, *Global hydrogen trade to meet the 1.5 climate goal: Part II - Technology review of hydrogen carriers*, International renewable energy agency, abu dhabi technical report, 2022.
98 A. Panagopoulos and K.-J. Haralambous, *Mar. Pollut. Bull.*, 2020, **161**, 111773.
99 A. Koutroulis, M. Grillakis, I. Daliakopoulos, I. Tsanis and D. Jacob, *J. Hydrology*, 2016, **532**, 16–28.
100 A. Gómez-Gotor, B. Del Ro-Gamero, I. P. Prado and A. Casanas, *Desalination*, 2018, **428**, 86–107.
101 UNESCO, *UN-Water, United Nations World Water Development Report 2020: Water and Climate Change, Paris*, UNESCO., UNESCO technical report, 2020.
102 L. Rosa, D. D. Chiarelli, M. C. Rulli, J. Dell'Angelo and P. D'Odorico, *Sci. Adv.*, 2020, **6**, eaaz6031.
103 L. Rosa, M. C. Rulli, K. F. Davis, D. D. Chiarelli, C. Passera and P. D'Odorico, *Environ. Res. Lett.*, 2018, **13**, 104002.
104 J. E. Lee, K.-J. Jeon, P. L. Show, S.-C. Jung, Y. J. Choi, G. H. Rhee, K.-Y. A. Lin and Y.-K. Park, *et al.*, *Fuel*, 2022, **308**, 122048.
105 M. F. Lagadec and A. Grimaud, *Nat. Mater.*, 2020, **19**, 1140–1150.
106 M. Chatenet, B. G. Pollet, D. R. Dekel, F. Dionigi, J. Deseure, P. Millet, R. D. Braatz, M. Z. Bazant, M. Eikerling and I. Staffell, *et al.*, *Chem. Soc. Rev.*, 2022.
107 N. Warwick, P. Griffiths, J. Keeble, A. Archibald, J. Pyle and K. Shine, *Atmospheric implications of increased Hydrogen use*, 2022, **https://www.gov.uk/government/publications/atmospheric-implications-of-increased-hydrogen-use**.
108 C. Antonini, K. Treyer, E. Moioli, C. Bauer, T. J. Schildhauer and M. Mazzotti, *Sustainable Energy Fuels*, 2021, **5**, 2602–2621.
109 L. Rosa and M. Mazzotti, *Renewable Sustainable Energy Rev.*, 2022, **157**, 112123.

